GL03855C

CHEMISTRY OF APOLLO 12 MARE BASALTS: MAGMA TYPES AND FRACTIONATION PROCESSES

by

J. M. Rhodes[1], D. P. Blanchard[2], M. A. Dungan[3], J. C. Brannon[1], and K. V. Rodgers[1]

[1]Lockheed Electronics Co., Inc., Houston, Texas 77058
[2]NASA-Johnson Space Center, Houston, Texas 77058
[3]NRC Research Associate, Johnson Space Center, Houston, Texas 77058

ABSTRACT

This paper presents major and trace element data for a large suite of petrographically diverse Apollo 12 mare basalts, and attempts to determine the number of magma types sampled at the Apollo 12 site, their compositional characteristics, their fractionation histories, and their spatial and temporal relationships. The new data confirm earlier classifications of these basalts into four compositional groups: the olivine, pigeonite, ilmenite and feldspathic basalts respectively. Two of these groups, the olivine and pigeonite basalts, are shown to be comagmatic, and related by olivine fractionation. The other groups differ in trace element and isotopic characteristics, and derived from different sources within the lunar interior.

An important consequence of this study is the recognition that the ilmenite basalts are a major basalt type, indigenous to the Apollo 12 site, and with a compositional range equivalent to that of the olivine-pigeonite basalts. The spatial relationships between these main basalt types are discussed in terms of local cratering events. It is suggested that the flows are thicker than the majority of lunar flows, and that the younger ilmenite basalts overlie the olivine-pigeonite basalts. The chemical variation within these basalt groups is attributed to extensive, olivine-dominated, near-surface crystal fractionation (about 30%), from parental magmas with compositions equivalent to the vitrophyres in each group, and to the formation of complementary olivine cumulates. There is a systematic relationship between inferred cooling rate and the position of a sample in the fractionation sequence. The more slowly cooled samples depart farthest from the parental magma composition, through both differentiation and cumulate processes.

INTRODUCTION

The Apollo 12 mission provided the first lunar samples that were readily understandable in terms of common terrestrial magmatic processes. Initial studies (e.g., LSPET 1970; Kushiro and Haramura, 1971) immediately recognized the importance of olivine fractionation in this texturally and chemically diverse suite of basalts. However, in detail the relationships proved to be somewhat less straightforward. Three major basaltic types were identified, largely on the basis of petrography and major element chemistry, and the internal variations within these groups were ascribed to near-surface fractionation (James and Wright, 1972). However, the trace element and isotopic variability was greater than could be expected from the fractionation of these three major basalt groups (Compston et al., 1971; Papanastassiou and Wasserburg, 1971), suggesting that multiple magma types, with similar major element chemistry but different trace element signatures, had been sampled.

Subsequent experience gained on mare basalts from other landing sites has shown that multiple magma types, erupted within narrow spatial and temporal limits, are a ubiquitous characteristic of mare volcanism (Chappell and Green, 1973; Rhodes and Hubbard, 1973; Helmke et al., 1973; Rhodes et al., 1976). Attempts to reconcile inferences based on major and trace element chemistry have met with varying success, but in general the trace element data imply greater complexity than is evident from petrography or fractionation trends derived from major element data.

In this paper we present major and trace element chemistry for a large, texturally diverse suite of Apollo 12 mare basalts.

We have attempted to integrate this information with petrographic inferences and with relevant experimental studies in an attempt to answer questions concerning the number of magma types at the Apollo 12 site, their spatial and temporal relationships, and their fractionation histories. In this attempt, we have benefited from a companion paper by Dungan and Brown (1977), which details the petrology and mineral chemistry of some of these samples. We have not concerned ourselves with the nature of the source of these basalts, or its evolution. This is the subject of a companion paper by Nyquist et al., (1977), which relates Rb-Sr geochronology for the same suite of samples to the evolution of the lunar interior and the source of mare basalts.

Major and trace element data for 20 Apollo 12 mare basalt samples are given in Table 1, and their petrographic characteristics are briefly outlined in Table 2. In both tables, the data are arranged according to chemically defined magma-types (as discussed below), and in decreasing atomic Mg/(Mg+Fe) values. For convenience, this ratio will be designated the Mg'-value throughout the paper. The major element data were obtained by x-ray fluorescence analysis following our customary procedures (Norrish and Hutton, 1969). Na, Hf, Sc, Cr, Co, Ni and REE element abundances were determined by instrumental neutron activation analysis (Jacobs et al., 1976), Sr, Y, Zr and Nb by x-ray fluorescence analysis (Norrish and Chappel, 1967), and Ba by stable isotope dilution mass spectrometry (Gast et al., 1970).

THE APOLLO 12 BASALTS

James and Wright (1972) identified three major basalt groups at the Apollo 12 site: olivine-pigeonite basalts, ilmenite-bearing basalts, and feldspathic basalts. This scheme has been adopted in the more recent attempts at mare basalt classification, with the exception that the pigeonite and olivine basalts are considered separately in recognition of the distinct compositional hiatus between them (Rhodes et al., 1975, Papike et al., 1976).

This study has doubled the number of basalts from the Apollo 12 site for which comprehensive chemical information is available, and has essentially confirmed the four basalt groups recognized in the previous studies. In constrast with earlier work, we have used trace as well as major element data to discriminate between the various basalt types, using a combination of realistic crystal fractionation models and trace element signatures. As in our Apollo 17 mare basalt study (Rhodes et al., 1976), we have emphasized fine-grained, rapidly-chilled samples to establish discriminatory criteria, on the assumption that these samples most closely approach magma compositions and are less likely to be subject to sampling problems. Coarser-grained samples are subsequently assigned to the appropriate basalt type according to the criteria established for finer-grained samples. Similarly, we rely on magmaphile element ratios in preference to their absolute abundances as discriminants among basalt types. Since these elements have low crystal/liquid distribution coefficients, their ratios are unlikely to be grossly perturbed by fractionation processes or by unrepresentative sampling of coarse-grained basalts. The most useful of these ratios are Ba/Sm and Ce/Sm, both

of which reflect the slope of the light rare-earth depletion, and also various combinations of such incompatible elements as Ba, Zr, Y, and Nb. Sc and Sr are useful discriminants, but their ratios to magmaphile elements tend to decrease in more evolved samples as a consequence of the onset of pyroxene and plagioclase fractionation. Table 3 summarizes some of the more useful discriminatory ratios for the four basalt groups, listing the "best-estimate" for each group based on the most rapidly chilled sample in the group, together with the range in the ratio found during this study. In order to minimize the effects of inter-laboratory bias we have included only data from this study in this compilation.

Fig. 1, a plot of the Ba/Sm ratio versus Mg'-value, serves to illustrate the relative constancy of such ratios within a basalt group over varying degrees of fractionation. An obvious feature of both this diagram and the ratios listed in Table 3 is the close correspondence in magmaphile element ratios of the olivine and pigeonite basalts: strong evidence for either a comagmatic origin or derivation by different amounts of partial melting from a common source. The ilmenite basalts are distinctly different from both the olivine and pigeonite groups, and must be derived from a separate parental magma and from a different source in the lunar interior. The necessity for a separate source is further emphasized by higher initial strontium isotope ratios in the olivine and pigeonite basalts than those of the ilmenite basalts (Fig. 2). The isotopic data in this figure are taken from the companion paper of Nyquist et al., (1977) and from Papanastassiou and Wasserburg (1971), and are plotted against TiO_2 content, a measure of crystal fractionation in both basalt groups.

An important consequence of this study is the recognition that the ilmenite basalts are an abundant and significant rock type at the Apollo 12 site. Previously, only four chemically analyzed samples could be assigned to this group (Papike et al., 1976), and one of these, 12064, should in fact be included with the pigeonite basalts on the basis of the criteria established in this paper. We now recognize ten samples of ilmenite basalts, spanning a wide compositional range from olivine-rich partial cumulates to highly evolved samples. In view of their abundance and broad compositional range, it seems more probable that they are indigenous to the site, rather than exotic fragments thrown in from a nearby "unsampled" basaltic unit as has been suggested by Pieters and McCord (1976). The ilmenite basalts range from olivine normative partial cumulates such as 12005, with the highest Mg'-value (0.61) of any mare basalt described to date, to highly-evolved quartz-normative samples (12047, 12054) with Mg'-values as low as 0.36 (Table 1). In terms of major element chemistry they are readily distinguished from the olivine and pigeonite basalts by lower SiO_2 and higher FeO and TiO_2 abundances for a given MgO value (Figs. 3-5). Similarly, the ilmenite basalts are enriched relative to the olivine and pigeonite basalts in most magmaphile elements, with the exception of barium, for a particular value of MgO (Figs. 6-8). In addition to a higher magmaphile element content, the ilmenite basalts display a pronounced depletion in the light rare-earths, which is reflected in lower Ba/Sm (Fig. 1) and Ce/Sm ratios than in the olivine and pigeonite basalts (Table 3). Thus ilmenite basalts appear to possess chemical characteristics that are intermediate between those of typical low TiO_2 basalts and high TiO_2 basalts from the Apollo 17

and 11 sites. There are exceptions to this general rule; for example, the Zr/Nb ratio (about 20) is too high to fall between typical low TiO_2 basalts (about 17) and high TiO_2 basalts (10-15) (Duncan et al., 1976). Sample 12036, although tentatively included with the ilmenite basalts, presents a special classificatory problem. It is too high in TiO_2, Sc and many magmaphile element abundances (Figs. 4-8) to be included with the olivine basalts, yet many of the element ratios (e.g., Ba/Sm + others) imply an affiliation with this group, whereas others (e.g., Ce/Sm) have intermediate values between the groups. Strontium isotopic data (Nyquist et al., 1977) do not resolve the problem, since these authors report an initial Sr 87/86 ratio of 0.69946, which is in between the majority of samples in the ilmenite and olivine-pigeonite groups (Fig. 2).

Our data for the olivine basalts fall within the range previously established for this group (James and Wright, 1972; Rhodes et al., 1975; Papike et al., 1976) and include an olivine vitrophyre (12015) which is both chemically and texturally similar to 12009, as well as several coarser-grained more olivine-rich samples. Sample 12006, which was classed as a feldspathic basalt by James and Wright (1972) solely on petrographic evidence, clearly belongs with these olivine-rich samples, on the basis of its composition, as its description in the Apollo 12 Lunar Sample Information Catalog (1970) would suggest. There is evidently a discrepancy for this sample between the thin section collection and the material allocated for our study.

All the olivine basalts contain both modal and normative olivine, and have high Mg'-values ranging from 0.49 in rapidly cooled vitrophyres such as 12009 and 12015 to 0.58 in more slowly cooled microgabbros such as 12035 and 12040 (Fig. 10).

As noted by Walker et al., (1976a), there is a strong correlation between grain size and the normative and modal olivine content. The olivine basalts are separated from the pigeonite basalts by a distinct compositional hiatus (Figs. 3-5) with the olivine basalts containing lower SiO_2, TiO_2, Al_2O_3, CaO and magmaphile element abundances and correspondingly higher amounts of MgO, Cr_2O_3, Co and Ni. The magmaphile element ratios in the two groups are essentially the same (Table 3), and they have identical relative rare-earth patterns that are less depleted in light rare-earths than the ilmenite basalt patterns.

Prior to this investigation, only four chemically analyzed pigeonite basalts were known (Papike et al., 1976) and the compositional range was small. Our new data (Table 1) extends both the number of samples in the group and the chemical variation, including samples (e.g., 12007, 12039) that are substantially evolved from the main cluster of compositions (Figs.3-5).All.the pigeonite basalts are quartz normative, with Mg'-values ranging from 0.43 in 12011, a rapidly-cooled sample, to 0.33 in 12039, a slowly-cooled and evolved member of the group. The evolved pigeonite basalts have high TiO_2 contents, and in fact their major element compositions converge on those of low Mg'-value samples in the ilmenite group (Figs.3-5)with which they are almost isochemical. They can, however, be readily resolved from the ilmenite basalts by several critical trace element ratios (Table 3) (e.g., Ba/Sm, Sc/Sm, Sr/Ba Zr/Nb) and by initial strontium isotope ratios (Nyquist et al., 1977). Sample 12064 has been assigned to the ilmenite basalts in previous studies on account of its high TiO_2 content of 3.99%. However, on the basis of high initial strontium 87/86 and Ba/Sm ratios it should be assigned to the pigeonite basalt group (Figs.1-2).

Similarly sample 12039, classed by James and Wright (1972) on petrographic evidence as an ilmenite basalt, should also be included with the pigeonite basalts.

Previously, only one sample of feldspathic basalt (12038) had been analyzed and its trace element characteristics (Compston et al., 1971; Schnetzler and Philpotts, 1971) are sufficiently different from the other basalts to exclude it from the three major basalt types. An additional sample 12031, originally classed as an ilmenite basalt by James and Wright (1972), is very similar to 12038 in major element chemistry, having high amounts of Al_2O_3, CaO and SiO_2 and correspondingly lower values of FeO and MgO. Both samples contain about 35-36 percent normative plagioclase, in contrast with the 27-29 percent common in the pigeonite basalts. Despite these major element similarities, 12031 differs from 12038 in its trace element characteristics and is similar to the olivine-pigeonite basalts (Table 3). It may be a plagioclase-enriched variant of the pigeonite basalts, either by plagioclase accumulation or by inadequate sampling of material that is heterogeneous at the hand-specimen level. However, the trace element ratios depart sufficiently from the "best estimates" for the pigeonite basalts to prevent unambiguous classification of this sample.

Table 4 assigns all currently analyzed Apollo 12 basalts to the appropriate basalt group, ranking them in order of inferred cooling rate. The cooling rate estimates are based on a variety of criteria including overall grain size, plagioclase size and morphology, the nature of the groundmass, and comparisons with experimentally determined cooling-rate studies on rocks of similar composition (e.g., Lofgren et al., 1974; Donaldson et al., 1975).

SPATIAL RELATIONSHIPS

Since almost all "hand-specimen" sized basalts collected at the Apollo 12 site have now been analyzed in detail and most can be assigned with confidence to the major basalt groups, it is appropriate to consider the spatial aspects of these basalt types and to attempt to infer their stratigraphic and temporal relationships. Fig. 9 is a sketch map of the Apollo 12 site, taken from Sutton and Schaber (1971), showing locations, where known, of all analyzed samples. It is readily apparent that the majority of the ilmenite basalts are located in the vicinity of Surveyor Crater in the S.E. part of the landing site, whereas the olivine basalts are largely confined to the N.W. section close to Middle Crescent Crater. The locations of several olivine basalts (12002, 12006, 12009, 12012, 12018, 12020) are not known with certainty, but they were all collected on EVA-1 somewhere between the LM and Middle Crescent Crater, four of them coming from the rim of the crater (Sutton and Schaber, 1971).

There is no apparent preferred distribution for the pigeonite basalts; they are found throughout the landing site. Sutton and Schaber (1971) show that continuous ejecta from the 400 m Middle Crescent Crater should cover the Apollo 12 landing site, and that this ejecta will have been reworked by the impacts creating Surveyor, Head and Bench Craters. Thus, the spatial distribution of samples may be depth related, controlled mainly by ejecta from Middle Crescent Crater, as originally suggested by Warner (1971). On this theory, the olivine basalts were excavated from the greatest depth and should be the oldest. The ilmenite basalts should be younger, overlying the olivine basalts, and the pigeonite basalts, if they are comagmatic with the olivine basalts as the chemical data suggests, are probably sandwiched between the olivine and ilmenite basalts.

If one applies the crater ejecta model of McGetchin et al., (1973) to Middle Crescent Crater it is clear that its ejecta blanket will only be a few meters thick, ranging from 8-10 m at the rim to only 1-2 m in the vicinity of Surveyor Crater. In view of the fact that Surveyor and Head Craters probably excavated material from about 40 to 20 m respectively, it seems unlikely that ejecta from Middle Crescent Crater will dominate the sample distribution throughout the site. The areal distribution can, however, be readily explained by assuming substantial thicknesses for the major basaltic types and that ilmenite basalts overlie older olivine basalts. Middle Crescent Crater, which probably excavated to a depth of about 80 m., sampled both olivine and ilmenite basalt. Olivine basalt,

which is ubiquitous at the rim-crest, will have been excavated from the greatest depth. On the other hand, Head and Surveyor Craters, which penetrated only to depths of about 20 and 40 m respectively, sampled both ilmenite and pigeonite basalt, but failed to penetrate the deeper olivine basalt. If this model is correct, it implies that the combined thickness of the ilmenite and pigeonite basalts must be substantial, possibly over 40 m thick. A similar thickness for the underlying, older olivine basalt is also required, probably between 30 and 50 m. Although lava flows up to 30 m thick have been described, apparently they are not common and have been ascribed to localized high rates of magma effusion (Schaber et al., 1976). Flow thicknesses of about 10 m or less appear to be more common in the mare basins (Howard et al., 1972; Schaber et al., 1976).

On the basis of plagioclase grain size and thermal Walker et al., (1976a) modeling, arrive at cooling unit thicknesses for the olivine basalts similar to those suggested here. They suggest that some of the coarse-grained olivine basalts crystallized at a distance of 11 m from the flow base, and that a flow thickness of at least 30 m would be required to maintain the appropriate cooling history. Since the coarsest of the ilmenite basalts compare closely in texture with the olivine basalt samples (Dungan and Brown, 1977), a similar cooling history may be implied and a comparable thickness for the ilmenite basalt cooling unit is not unlikely.

CRYSTAL FRACTIONATION

It has been widely recognized that near-surface crystal fractionation has played a major role in the evolution of the Apollo 12 mare basalts (e.g. LSPET, 1970; Kushiro and Haramura, 1971; Compston et al., 1971; Green et al., 1971a; James and Wright, 1972; Walker et al., 1976a). The olivine and pigeonite basalts were regarded as comagmatic, the compositional variation being controlled primarily by olivine fractionation; but the relationships for the ilmenite basalts were obscure. The new data presented in this paper allows us to re-examine these relations in greater detail. Specifically, we are concerned with the nature and number of parental magmas involved; with the magmatic history of the ilmenite basalts; and with the fractionation history of the olivine basalts, and their relationship to the pigeonite basalts.

In a detailed chemical study, Compston et al., (1971) argued that the Apollo 12 basalts were derivatives from at least six parental magmas, each associated with a separate episode of partial melting in the lunar interior. Primary evidence for this was the wide variation in Rb/Sr ratios and also the variation in magmaphile element abundances that could not be quantitatively accounted for by crystal fractionation models consistent with the major element data. The wide spread in initial strontium isotope ratios also implied that multiple magma types had been sampled (Papanastassiou and Wasserburg, 1971). This conflict between large variances in the trace element data and the relatively simple crystal fractionation models implied by the covariance of the major element data, is a common problem in both lunar and terrestrial basalt petrogenesis.

It has been widely interpreted as implying several parental basaltic magmas with distinctive trace element signatures, that follow essentially identical liquid lines of descent at the Apollo 15 (Helmke et al., 1973) and at the Apollo 17 (Shih et al., 1975) site, as well as at the Apollo 12 site. Several factors impede the resolution of this problem:

1) Inter-laboratory bias in trace element determinations. This is probably the least troublesome.
2) Most of the magmaphile elements used to distinguish between parental magmas and their associated derivatives are concentrated in the mesostasis. Consequently, their determination can be subject to severe sampling problems. This is particularly true for coarse-grained rocks. For example, our measurements of rare-earth elements in 12039 differ from those reported by Nyquist et al., (1977), on a different sub-sample, by a factor of 1.2. This is not an inter-laboratory bias since barium measurements on the two sub-samples in one laboratory show the same discrepancy.

Clearly, it is dangerous to infer the existence of distinct magma-types solely on differences in magmaphile element abundances. A safer approach is the use of element ratios, as discussed earlier, on the assumption that they are less likely to be disturbed by inadequate sampling than are the absolute / abundances. The drawback to using element ratios is that although it is possible to distinguish magmas that are derived from different sources, it is difficult to resolve those magmas that are produced by varying amounts of melting from the same source, since the ratios will tend to remain the same. The only satisfactory solution to this dilemma is to rely heavily on fine-grained, rapidly chilled samples for evidence, or on suites

of coarser-grained samples that exhibit systematic covariance with the major element data. Single coarse-grained samples that depart from such covariant trends are not sufficient evidence for the deduction of different magma types.

3) By definition, magmaphile elements are excluded from the major rock-forming minerals and are concentrated in the residual liquids. It appears to us intrinsically probable that during the slow cooling of sizeable lava flows, this residual liquid will be mobilized, resulting in zones that are enriched or depleted in magmaphile elements, independent of the major element chemistry. Such a case has been documented in detail by Hart et al., (1971) for a single 10 m Icelandic lava flow, and Rhodes et al., (1976) explained the systematic magmaphile element depletion of several coarse-grained Apollo 17 basalts relative to fine-grained basalts having similar magmaphile element ratios, by this process. Again, the departure of absolute magmaphile element abundances from those predicted by major element fractionation trends may lead to erroneous conclusions concerning the number of magma-types necessary to account for trace element variance, and the use of element ratios or data from rapidly-cooled samples is to be preferred.

From the preceding discussion, it is clear that much of the diversity in trace element abundances in Apollo 12 basalts, and their departure from well-established major element fractionation trends, may result from a variety of causes. It is perhaps premature to advocate the existence of multiple magma types until all other possibilities can be excluded.

When we examine the Apollo 12 data in the light of the preceding discussion, emphasizing our own data to alleviate inter-laboratory bias, we arrive at the following conclusions:

1) The major element data establish two well-defined fractionation trends for the olivine-pigeonite and ilmenite basalt groups. The feldspathic basalts 12038 and 12031 may be related to these basalts by plagioclase accumulation processes, but the evidence is ambiguous.

2) There are several rapidly-chilled vitrophyres possessing almost identical Mg'-values and MgO, Cr_2O_3 and Co abundances (e.g., 12008, 12009, 12015, 12045). These samples are distinctly bi-modal in their abundances and ratios of many magmaphile elements, corresponding to the olivine (12009, 12015) and ilmenite (12008, 12045) basalt groups (Table 3, Fig. 1).

3) The coarser-grained samples reflect the same bi-modal distributions in magmaphile element ratios (Table 3, Fig. 1), and although there is appreciable scatter, the magmaphile element abundances are broadly covariant with the major element trends (Figs. 6-8).

4) The initial strontium 87/86 data are also bi-modal (Nyquist et al., 1977) with the olivine-pigeonite basalts possessing higher ratios than the ilmenite basalts. There are some samples with intermediate values, and suggestions of sub-groups within the data. However, the uncertainties are such that they cannot be resolved from the main groups.

Thus, with the exception of sample 12038, there is no compelling evidence for more than two major magma types at the Apollo 12 site: the olivine-pigeonite and the ilmenite basalts. With this established, we can discuss the nature of the parental magmas and their fractionation histories in more detail.

The Olivine-Pigeonite Basalts

Olivine-controlled crystal fractionation has been extensively documented for the olivine and pigeonite basalts (e.g. Kushiro and Haramura, 1971; Compston et al., 1971; James and Wright, 1972). The data in Table 1 confirm these observations, following well-defined trends of increasing SiO_2, TiO_2, Al_2O_3 and CaO with decreasing MgO and Cr_2O_3 (Figs. 3-5). Table 1 lists the data in order of decreasing Mg'-value, and it is readily seen that there are similar progressive and systematic changes in major and trace element abundances, and in normative olivine or quartz content. Such variations are consistent with crystal fractionation dominated by ferromagnesian minerals. Fig. 10 attempts to summarize the relative positions of the samples in the fractionation sequence, and to integrate this with inferences concerning their cooling history. This diagram will be used as a framework for further discussion of the fractionation of these rocks. The Mg'-value is used as a fractionation index, and, within a particular interval, essentially isochemical samples are ranked according to their relative cooling rate. Samples that differ in composition but are inferred to have had similar cooling histories are placed at the same level. Cooling rate estimates are based on examination of the curatorial thin section collection, and are influenced by a variety of criteria, including overall grain size, plagioclase size (Walker et al., 1976a) and morphology (Donaldson et al., 1975; Lofgren et al., 1974).

Although necessarily subjective, our ranking for the olivine-normative basalts, corresponds closely with similar cooling rate evaluations of Donaldson et al., (1975) and Walker et al., (1976a). In Fig. 10 samples discussed in this paper are included in a heavy outlined box. Included with the sample number is the normative olivine or quartz content and the ratio of Ba in the sample to its concentration in the inferred parental magma. Both factors provide independent estimates of the degree of fractionation, and for most samples there is good agreement between these estimates and the relative position in the sequence based on the Mg'-value.

It is evident from Fig. 10 that there are two contrasting cooling rate trends within the olivine-pigeonite basalt series. The olivine basalts display an inverse relationship between cooling rate and Mg'-value: that is, the more slowly cooled samples are richer in normative olivine. This relationship has been discussed in detail by Walker et al., (1976a), and attributed to olivine accumulation at the base of a single flow. Conversely, there is a positive correlation between cooling rate and Mg'-value in the pigeonite basalts, fractionation having proceeded further in the more slowly cooled samples. Within the olivine basalts there are two subgroups, separated by a hiatus in the Mg'-value between 0.52 and 0.54 (Fig. 1). Samples with Mg'-values less than 0.52 (12009, 12015, 12004, 12076) have all cooled quickly and are closely comparable in composition. Two of these (12009, 12015) are vitrophyres, and must have been erupted onto the lunar surface as liquids, or liquids bearing a small percentage of olivine phenocrysts. Green (1971b) has argued that the composition of 12009 (Mg'-value 0.49) is close to that of the immediate parental magma for

this suite of rocks. Several lines of evidence indicate that this is a realistic assumption, perhaps erring towards low Mg'-values:

1) The most magnesium-rich olivine composition reported for Apollo 12 mare basalts is Fo_{77} (Butler, 1972), which according to the Roeder and Emslie (1970) Fe/Mg distribution between olivine and melt, would indicate crystallization from a magma with an Mg'-value of 0.52.

2) Donaldson et al., (1975) suggest, on the basis of experimentally determined textural evidence, that some of 12009 olivine crystallized slowly prior to eruption, and that 12009 was extruded onto the lunar surface bearing a small percentage of olivine phenocrysts.

3) The hiatus in Mg'-values between 0.52 and 0.54 has been interpreted by Papike et al., (1976) as being indicative of the value for a magma parental to the Apollo 12 basalts.

4) There is strong evidence, both textural and experimental (e.g., Green et al., 1971a, Walker et al., 1976a,b) that the samples with Mg'-values greater than 0.54 are olivine-enriched partial cumulates, thereby limiting the parental magma composition to an Mg'-value of less than 0.54.

In view of the close limits that can be placed on the composition of the inferred parental magma for the olivine basalts, we shall adopt the vitrophyre 12015 as the parental composition in the following discussion.

The suggestion that samples with Mg'-values higher than those of the vitrophyres must be olivine-enriched partial cumulates receives strong support from three areas: Firstly, it has been shown that the major element compositions of these samples can be modeled simply by adding olivine and minor Cr-spinel to the inferred magma

composition (e.g., Kushiro and Haramura, 1971; Compston et al., 1971); secondly, Green et al., (1971a) and Walker et al., (1976b) argue that the fact that the experimentally determined liquidus olivines in these samples are more forsteritic than the most magnesian cores in the basalts indicates olivine accumulation; thirdly, the inverse relationship between cooling rate and normative olivine content, or Mg'-value, seen in Fig.10 has been shown by Walker et al., (1976a) to be consistent with olivine settling in the basal part of a 30 m cooling unit, where the amount of cumulus olivine increases upwards with decreasing cooling rate and increasing grain size.

Starting with a parental magma of 12015 composition, basalts with Mg'-values greater than 0.54 can be derived by varying amounts of olivine (Fo72) (± Cr-spinel) accumulation into the parental magma. Calculations indicate that sample 12014 requires about 6 percent olivine accumulation, whereas sample 12006 requires about 12 percent.

Inspection of Figures 3 to 8 shows that there is reasonable consistency between major and trace element estimates in the amount of olivine accumulation required for these rocks. The "best-fit" olivine (Fo72) required to account for these compositional variations is less forsteritic than experimentally determined liquidus olivines (Fo75-78) in melts compositionally close to the inferred parental magma (Green 1971b; Walker et al. 1976b) or than the most forsteritic cores (Fo77) observed in rapidly chilled rocks. The majority of phenocryst cores are less forsteritic than either of these, about Fo69-71 (Butler, 1972). This is closer to the composition required to account for the fractionation trends, and presumably results from re-equilibration with the melt on cooling over a substantial temperature interval below the liquidus (Green, 1971b; Walker et al., 1976b).

Major element data from the literature (Compston et al., 1971; Kushiro and Haramura, 1971; Willis et al., 1971) indicate that the majority of the other high Mg'-value samples have accumulated similar amounts of olivine, about 8 to 15 percent, together with minor spinel. Two samples, 12035 and 12040, are more extreme examples, requiring about 20 percent olivine accumulation (Figs.3,4). The trace element data for these coarse-grained olivine-enriched samples are highly variable, departing significantly from the calculated olivine accumulation trend. Nevertheless, because their trace element ratios and major element compositions are consistent with derivation from a magma of 12015 composition, we prefer to regard them as partial cumulates from this magma rather than derivatives from some unspecified and unsampled magma. These samples are all coarse-grained, have cooled slowly (Fig. 10), and have had abundant opportunity for re-equilibration and migration of intergranular, trace element-enriched, residual fluids. Sample 12036 may be one extreme example of this type of process. It is clearly olivine-enriched and could have been derived by about 20 percent olivine accumulation from a magma with an Mg'-value of 0.50. However, we are not clear from which, if any, of the two parental magma types it is derived. If it is derived from the 12015 composition, as some of its elemental ratios and strontium isotope ratios seem to imply (Fig.1,2), it has been enriched substantially in TiO_2 and other magmaphile elements.

If the cooling model proposed by Walker et al., (1976a) for the olivine basalts is essentially correct and they have accumulated within a sizeable flow, complementary differentiates must exist within that cooling unit. The quartz-normative pigeonite basalts, with Mg'-values extending from 0.43 to 0.33, are obvious contenders for this role. We have seen previously that rapidly-cooled members of the olivine and

pigeonite basalt groups have almost identical magmaphile element ratios (Table 3), indicating either that they are comagmatic or that they were derived from a common source. Earlier studies (e.g., Compston et al., 1971; Kushiro and Haramura, 1971; James and Wright, 1972) have shown that the compositions of the few pigeonite basalts then analyzed fall on olivine control lines from the olivine basalts, indicating that both basalt types could have been derived from a common magma. Later reviews (Rhodes et al., 1975; Papike et al., 1976), impressed by the compositional hiatus between the two basalt types and the wide variations in trace element chemistry, have treated them separately although recognizing their potential comagmatic nature.

Sample 12011 is the least evolved (Mg'=0.43) of the pigeonite basalts. It is also the most rapidly cooled, with a fine-grained, variolitic, groundmass containing phenocrysts of pigeonite and skeletal microphenocrysts of olivine. It is an ideal sample to test for relationships between the olivine and pigeonite basalts, since sampling problems should be minimal, and there should have been no opportunity for migration of residual liquid. Least squares calculations indicate that the 12011 major element composition can be very closely matched by the removal of 15 percent olivine (Fo72) and 0.4 percent Cr-spinel from a 12015 magma composition. These are, of course, the petrographically observed and experimentally

determined liquidus phases over a wide temperature interval in the olivine vitrophyres (Green, 1971b), and are the phases necessary to produce the olivine-enriched samples. Since the olivine/liquid distribution coefficients for the magmaphile trace elements are low (<0.02), the ratio of the concentration in the parent magma to its concentration in the derivative magma provides an estimate of the amount of liquid remaining (Anderson and Greenland, 1969). Using this relationship, we find that for most of these elements (e.g., Ba, Sr, Zr, Sm, Lu) the extent of fractionation varies between 14 and 16 percent, in excellent agreement with the independent estimate based on major element data. Similarly, by using $D^{oliv/liq} = 3$ and an initial cobalt concentration of 51 ppm in a parental magma of 12015 composition, we can show that 15 percent olivine fractionation should decrease the cobalt concentration to 37 ppm, again, in excellent agreement with the 39 ppm found in 12011. Thus, there can be little doubt that the pigeonite basalts are comagmatic, evolved derivatives of the olivine basalt.

Other, more evolved, members of the pigeonite basalt group (12043, 12017, 12055) continue this olivine fraction trend, requiring, respectively, the removal of 17.5, 17.7 and 18.4 percent olivine (Fo72) and 0.5 percent Cr-spinel from a magma with the composition of 12015. The trace element data (Figs.6-8) indicate similar amounts of olivine and spinel fractionation, up to 20 percent, but the internal consistency in these coarser-grained samples is not as satisfactory as that observed for the 12015-12011 relationship. After about 20 percent olivine + spinel fractionation, olivine is no longer observed and when the magma has reached an Mg'-value of about 0.40 /pigeonite becomes the dominant fractionating phase. This results in marked departure from the olivine fractionation

trends with an increase in TiO_2 and magmaphile elements and decrease in SiO_2, with relatively little change in the MgO content (Figs.3-8). Similar trends are observed in the experimentally determined liquid line of descent for 12002 (Walker et al., 1976b), at the onset of pigeonite crystallization. The three most evolved of the pigeonite basalts, 12064, 12007 and 12039, with Mg' values of 0.37, 0.35 and 0.33 respectively, show evidence of substantial pigeonite fractionation. Attempts to model this stage in the fractionation process are not as satisfactory quantitatively as were the results for the earlier olivine fractionation, presumably because these are slowly cooled samples (Fig. 10), and will have had abundant opportunity for re-equilibration and migration of residual liquid, thus complicating the fractionation process. Furthermore, as we discussed earlier, sampling of coarse-grained samples, such as 12039, is a problem as evidenced by the 20 percent difference in rare-earth elements found in different sub-samples of this rock. Nevertheless, there is sufficient consistency between the major and trace element data to indicate that these samples result from about 30 to 35 percent fractionation from a magma of 12015 composition, and that the later stages of this process are controlled by pigeonite. For example, major element calculations indicate that 12007 can be derived from a melt corresponding to the pigeonite basalt 12011 by removal of about 10 percent pigeonite and 3 percent olivine (Fo66). Similarly, 12039 requires the removal of 17 percent pigeonite and only 1.5 percent olivine, but also 4 percent plagioclase (An95). The magmaphile element abundances are generally supportive of these calculations, since, in Figs. 6-8 , these samples plot closer to the pigeonite control line than to the olivine one. Furthermore, the amount of

fractionation from the parental magma composition of 12015 indicated by the magmaphile elements is between 29 and 33 percent for 12007 and 29 and 35 percent for 12039, in comparison with 28 and 38 percent calculated from major element data.

In the experimental equilibrium crystallization studies on 12002 of Walker et al., (1976b), pigeonite is followed within 20°C by plagioclase in the crystallization sequence. Thus, we might expect to see the effects of plagioclase fractionation in samples that reflect more than 30 percent fractionation. Sample 12039 is depleted in strontium relative to 12007 and the pigeonite fractionation trend, which is qualitative support for the major element calculations that require some plagioclase removal to generate this composition from a magma comparable to 12011. Sample 12031 is remarkably similar to 12038 in major element chemistry, and both are enriched in plagioclase relative to other Apollo 12 basalts. However, 12038 is distinctly different from other Apollo 12 basalts in its trace element abundances and their ratios, whereas 12031 is not. Many of the magmaphile element ratios, with the exception of those that would be modified by plagioclase fractionation, are similar to those for the olivine and pigeonite basalts (Table 3). However, the SiO_2 content is far too high for this sample to be a plagioclase-enriched derivative of the pigeonite basalts. Its relationships are an enigma; perhaps it is another example of inadequate sampling?

In the preceding discussion, we have argued that the olivine and pigeonite basalts are comagmatic; that fractional crystallization of a parental magma compositionally equivalent to the olivine vitrophyres gave rise to olivine-enriched samples, resulting

from 10-20 percent olivine accumulation; that the same parental magma produced the evolved pigeonite basalts from 15 to more than 30 percent crystal fractionation, initially dominated by olivine, but subsequently by pigeonite and possibly plagioclase.

Although the genetic relationships can be firmly established, the spatial relationships present certain problems. In the case of a single differentiated cooling unit, the pigeonite basalts would be the complementary differentiates to the olivine-enriched basalts that are inferred to have formed at the base of a thick cooling unit (Walker et al., 1976a). The marked relationship between cooling rate and degree of fractionation, evident in Fig. 10, for the pigeonite basalts, would suggest that these samples were from the upper half of the cooling unit, where such a relationship would be expected to hold. Although this model is appealing in its simplicity, two additional lines of evidence suggest that the relationships could be more complicated. First, the rapidly chilled pigeonite basalt 12011 must have crystallized very close to the surface of a cooling unit. This is unlikely in the case of a single differentiated flow, since olivine vitrophyres would crystallize at the upper surface. Secondly, the compositional hiatus between the olivine and pigeonite basalts should not exist in a single differentiated flow. It is in fact suggestive of a two-stage history involving sub-surface crystallization of olivine basalt, followed by the subsequent eruption of a separate pigeonite basalt flow. In this case, the correlation between decreasing cooling rate and progressive fractionation in the pigeonite basalts would reflect sampling of the upper part of this flow. A possible way out of the dilemma, since there must be complementary differentiates to the

basalts,
olivine-enriched / is to suggest that a single thick basalt flow, initially of olivine vitrophyre composition, fractured during differentiation and was breached by the evolved pigeonite basalt magma.

The Ilmenite Basalts

Prior to this study, only four ilmenite basalts had been chemically analyzed (Rhodes et al., 1975; Papike et al., 1976), and one of these (12064) is in fact an evolved pigeonite basalt. The seven additional samples of this basalt type, whose analyses are reported in Table 1, reveal a wide compositional range comparable to that of the olivine-pigeonite basalts, from an olivine-rich basalt with an Mg'-value of 0.61 to evolved quartz-normative basalts with Mg'-values as low as 0.36. As was the case with the olivine-pigeonite basalts, the ilmenite basalts follow well-defined trends of increasing SiO_2, Al_2O_3, CaO and magmaphile element abundances with decreasing MgO and Cr_2O_3 content (Figs. 3-5). Table 1 lists the samples in order of decreasing Mg'-value, which generally corresponds with systematic changes in other element abundances, and in normative olivine and quartz content. These trends are indicative of substantial amounts of crystal fractionation involving ferromagnesian minerals. Fig. 11 relates the inferred cooling history of the samples to their relative positions in the fractionation sequence. As was noted for the olivine-pigeonite basalts, there are two contrasting trends: the majority of samples reflect a correlation between cooling rate and the amount of differentiation, but the samples with high Mg'-values show an inverse relationship between cooling rate and position in the differentiation sequence. As is elaborated by Dungan and Brown (1977), these two contrasting / trends can be, conceptually at least, related to complementary accumulation / and differentiation processes occurring in a single cooling unit.

Sample 12008, a vitrophyre, is the most rapidly cooled of the ilmenite basalts. Texturally it resembles 12009, containing both equant and skeletal olivine phenocrysts. It can be presumed to have undergone a similar cooling history, and must have been erupted onto the lunar surface as either a liquid, or a liquid bearing a small percentage of pre-eruptive olivine phenocrysts (Dungan and Brown, 1977). Since it is also the least evolved of the ilmenite basalts (Mg'-value = 0.51) other than those of accumulative / origin (e.g., 12005), it provides the best available estimate of the parental magma composition for the ilmenite basalts. This suggestion gains further support from two other areas: first, the most magnesian olivine recorded in the ilmenite basalts is Fo76 in 12022 (Weill / et al., 1971), which according to Fe/Mg partitioning between olivine and liquid (Roeder and Emslie, 1970) would be the liquidus olivine for a magma with an Mg'-value of 0.51, such as 12008; secondly, the Mg'-value (0.51), Cr_2O_3 (0.61%) and Co (51 ppm) content of 12008 are all indicative of the "primitive"nature of the sample and are remarkably similar to the values for these variables in 12015, the inferred parental magma composition for the olivine-pigeonite basalts. In view of this evidence, we have adopted the vitrophyre 12008 as the composition of the parental magma for the ilmenite basalts.

Inspection of Figs.3-5 show that, to a first approximation, much of the compositional variation can be accounted for by olivine (Fo72) fractionation of a magma compositionally equivalent to 12008. Green et al., (1971a) show that for 12022, a rock whose composition is close to that of 12008, olivine is the liquidus phase over a wide temperature range, joined at 125°C below the liquidus by spinel, pigeonite and plagioclase in that order. The majority of the olivine

phenocrysts in 12008 fall within the narrow limits of Fo_{69-72} (Dungan and Brown 1977), which is in the range Fo_{77-65} reported by Green et al. (1971a) for experimental studies on 12022 prior to the onset of pyroxene crystallization. Consequently, the fractionation trend, dominated by olivine (Fo_{72}) is consistent with what one would expect from experimental and petrographic observations.

Although there is a general correspondence between sample compositions and the predicted olivine fractionation trends, several of the more slowly cooled samples show significant correlated departures from these trends for TiO_2 and the magmaphile elements. We attribute this to a greater potential for re-equilibration and migration of trace element enriched residual liquids in slowly cooled samples. A consequence of this process is that although magmaphile element ratios should remain essentially constant, and therefore characteristic of the ilmenite basalt group, their variable abundances will lead to inconsistencies in the amount of fractionation estimated from major and trace element-data. Some samples (e.g., 12056, 12016) are enriched in these magmaphile elements relative to what one would predict from the olivine fractionation model, whereas others (e.g., 12054, 12047) are depleted.

Given this apparent mobility in the magmaphile elements, it is useful to establish certain guidelines for examination of the fractionation process:

1) Although absolute abundances of the magmaphile elements may depart from a predicted fractionation trend, their ratios should reflect those of the ilmenite basalts (Table 3).

2) Strontium, europium and barium, elements that would be incorporated in preference to other magmaphile elements in late forming

plagioclase, should show less deviation from the olivine fractionation trends than other magmaphile elements. Inspection of Figs.6,8 shows that this is generally the case.

3) Since TiO_2 behaves as a magmaphile element in these basalts, it should also depart from the olivine fractionation trends.

We find this to be the case for those samples that are most strongly depleted in magmaphile elements. Since fractionation of late-stage ilmenite appears to be an implausible mechanism, and since ilmenite fractionation alone will not account for the correlated depletion in magmaphile elements, we attribute this variation to migration, by processes such as filter pressing, of a residual liquid rich in titanium and magmaphile elements.

4) Although the magmaphile elements cannot be used as an independent check of the major element modeling, ferromagnesian trace elements such as cobalt or nickel can. If we take the firmly established derivation of 12011 from 12015 by 15 percent olivine fractionation, we can use this data to calculate an effective olivine/liquid distribution coefficient for cobalt of 2.65. This can then be applied to the ilmenite basalts as an independent check of the major element estimates of olivine fractionation.

Samples 12045 and 12022 have cooled a little more slowly than 12008 and have slightly more evolved compositions (Fig. 11). Calculations show that the major element compositions of these two samples can be closely matched by the removal from a magma of 12008 composition of 2.6 and 7.0 percent olivine (Fo_{72}) respectively and 0.3 percent Cr-spinel (Figs.3-5). The trace element data are consistent with this estimate, requiring between 2 and 4 percent fractionation, as can be seen in Figs.6-8 .

Sample 12056 has cooled more slowly than the preceding samples, and has a consequence evolved to a greater extent. It can be derived from a magma of 12008 composition by removal of 12.5 percent olivine (Fo_{73}) and 0.3 percent Cr-spinel (Figs. 3-5). This sample is slightly enriched in all magmaphile elements relative to the calculated olivine fractionation trends (Figs. 6-8), with the result that predictions based on these elements would require greater degrees of olivine fractionation than is indicated by the major element data. Cobalt provides an independent check on the major element estimate since by using $D^{ol/lq} = 2.65$, the calculated Co content of a magma derived from a magma of 12008 composition by 12.5 percent olivine fractionation would be 41 ppm. This is close to the observed abundance of 42 ppm in 12056.

The inferred migration of magmaphile elements is more pronounced in 12047 and 12054, the most evolved of the ilmenite basalts (Fig. 11). These two samples are depleted in titanium and most magmaphile elements, with the exception of strontium and barium, relative to the theoretical fractionation trends (Figs. 4-8). The major element data can be modeled in a two step process, by olivine (Fo_{72}) and spinel fractionation to the 12056 composition, and then by the removal of iron-rich olivine (Fo_{60-66}), minor Cr-spinel and ilmenite. The necessity for fractionation involving more iron-rich olivine at these evolved compositions is consistent with one atmosphere melting experiments on 12022 (Green et al., 1971a) where the olivine at the olivine-pyroxene-plagioclase cotectic is Fo_{65}. The necessity for ilmenite fractionation is a consequence of the decrease in TiO_2 in these samples (Figs.4,5),

which we attribute to movement of a titanium-rich / residual liquid rather than the actual physical separation of ilmenite. If one accepts this interpretation, the major element data would then indicate that 12047 and 12054 resulted from 25 and 27 percent olivine and minor Cr-spinel fractionation from a magma of 12008 composition, and that the olivine removed became progressively less forsteritic (Fo_{72-60}) as fractionation progressed. Cobalt abundances provide an independent check of this model, the calculated amounts remaining in the magma after 25 and 27 percent olivine fractionation being 31.6 and 30.1 ppm respectively compared to measured values of 32 and 31 ppm.

In summary, then, we propose that starting with a parental magma compositionally equivalent to 12008, varying amounts of olivine (Fo_{72-60}) and spinel fractionation have taken place, ranging from as little as 2 percent in rapidly chilled rocks (12045), up to 27 percent in more slowly cooled samples. Dungan and Brown (1977) argue that it is only in slowly cooled magmas that such extensive olivine fractionation can occur, and suggest that the unfractionated / samples could have been derived from the upper surface of a single flow, with the more fractionated and slowly cooled samples located stratigraphically beneath those that are rapidly chilled. It follows, then, that at deeper levels in the flow olivine accumulation / must occur. Two samples from the ilmenite basalt group, 12005 and possibly 12036 meet this requirement. Sample 12016, another slowly cooled sample, does not differ greatly in major element composition from 12008, but its trace element abundances are rather erratic. Dungan and Brown (1977) indicate that this sample has undergone substantial re-equilibration,

and suggest that it has had a complex crystallization history, such as loss of olivine coupled with a compensatory gain of more iron-rich olivine from higher levels in the cooling unit. The relationships for 12036 are even more / nebulous. We have noted earlied that many of its magmaphile element ratios, suggest a genetic relationship to the olivine basalts (Fig. 1). On the other hand, it is too high in magmaphile elements to be related to these basalts without abundant enrichment in late-stage residual fluids. Furthermore, the major element composition can be derived successfully from 12008 by addition of olivine (14% Fo_{72}), pigeonite (8.7%), augite (3.5%), and minor Cr-spinel (0.3%). Similar calculations using 12015 as a parental liquid are not as successful. The necessity to include pyroxene as well as olivine in the calculations does not imply that both phases were co-precipitating, merely that substantial amounts of post-crystallization re-equilibration has taken place, involving cumulus olivine and the residual liquid.

Sample 12005 is the only clear example of olivine-enrichment / in the ilmenite basalts. It has an Mg'-value of 0.61, and is the most mafic of all lunar mare basalts. It has cooled very slowly (Fig. 11), commensurate with its high normative olivine content (42%) which is indicative of extensive olivine accumulation. By analogy with the models of Walker et al., (1976a), we attribute this to olivine settling near the base of the ilmenite basalt cooling unit. Calculations show that 12005 can be derived from a parental magma of 12008 composition by accumulation of 30 percent olivine (Fo_{72}), 3 percent pigeonite, 4 percent augite and 0.5 percent Cr-spinel (Figs. 3-5). As discussed above for 12036, we attribute the necessity for pyroxene to reaction relationship between the cumulus olivine and the residual liquid.

CONCLUSIONS

(1) This study has doubled the amount of compositional data available for the Apollo 12 basalts. It confirms the four basalt types identified in previous studies: the olivine, pigeonite, ilmenite and feldspathic basalts. The pigeonite basalts are shown to be comagmatic with the olivine basalts, derived from a common parental magma by substantial amounts (>15%) of olivine fractionation. The ilmenite basalts are compositionally distinct from the olivine-pigeonite basalts, and derive from a separate parental magma. We infer, on the basis of initial strontium isotope ratios and significant differences in many magmaphile element ratios, that the parental magmas for these major basalt types are derived by partial melting of distinctly different source material in the lunar interior. The relationship of the feldspathic basalts to the olivine-pigeonite and ilmenite basalts is enigmatic, and their paucity in the sample collection may imply that they are exotic to the area.

(2) The new data indicate that the ilmenite basalts are an abundant and important magma type at the Apollo 12 site. They are texturally and chemically varied, and, like the olivine-pigeonite basalts, reflect a wide range in cooling history and magmatic evolution. In both the olivine-pigeonite and ilmenite basalts this range includes rapidly cooled vitrophyres that we suggest are compositionally close to the parental magmas, and more slowly cooled evolved derivatives and complementary olivine-enriched accumulative basalts. There is a systematic relationship in both basalt groups between inferred cooling rate and position of a sample within the fractionation sequence. Departure from the initial parental magma composition

either through differentiation or cumulate processes is most pronounced in those samples that have cooled slowly. We deduce from this that the extensive fractionation displayed by both of these Apollo 12 basalt types is a consequence of crystallization in thick cooling units. The spatial relationships of the samples relative to local cratering events provide corroborative evidence for this assumption, and can be interpreted as indicating that a thick flow (40 m.) of ilmenite basalt overlays an older flow of equally thick olivine-pigeonite basalt.

(3) The compositional variation within both the olivine-pigeonite basalts and the ilmenite basalts is extensive, and for each it can be modeled largely in terms of olivine fractionation within a single cooling unit. Olivine (Fo_{72}) plus minor Cr-spinel fractionation in the olivine basalt parental magma (equivalent in composition to 12015) has led to the formation of olivine-rich basalts, containing between 10 and 20 percent cumulus olivine, and complementary, evolved pigeonite basalt magmas. With further fractionation, pigeonite replaces olivine as the dominant fractionating phase, producing evolved magma compositions that result from removal of about 30 percent of the combined phenocryst phases. A similar pattern of fractionation is followed by the ilmenite basalts, producing olivine-rich variants, with up to 30 percent cumulus olivine, and evolved differentiates that result from over 30 percent olivine (Fo_{60-72}) plus minor spinel fractionation.

(4) In some of the more slowly cooled rocks magmaphile element abundances depart significantly from crystal/liquid fractionation trends based largely on major element data and involving petrographically observed and experimentally

determined phenocryst phases. On the other hand, in rapidly chilled vitrophyres or variolitic samples, the major and trace element data provide self-consistent models of crystal/liquid fractionation that are realistic in terms of petrology and experimental studies. Sampling problems are a possible cause of the inconsistency in the coarse-grained samples. However, this inconsistency could also be produced by late-stage migration of magmaphile element-enriched residual liquids within slowly cooled magma bodies, resulting from mechanisms such as filter pressing. We believe that the mobilization of residual fluids is an intrinsically probable process that has been neglected in geochemical studies.

Acknowledgements — We wish to thank H. Wiesmann for providing isotope dilution barium determinations. Interchange of data and ideas with L. Nyquist proved to be most fruitful. Careful reviews by J. Green and G. Lofgren provided helpful advice and comments. Special thanks are due to L. Romero and C. Rhodes for assistance in preparation of the manuscript.

REFERENCES

Anderson A. T. and Greenland L. P. (1969) Phosphorus fractionation diagram as a quantitative indicator of crystallization differentiation of basaltic liquids. Geochim. Cosmochim. Acta 33, 493-505.

Apollo 12 Lunar Sample Information (1970) NASA publication TR R-353.

Apollo 12 Preliminary Science Report (1970) NASA publication SP-235.

Butler P., Jr. (1972) Compositional characteristics of olivines from Apollo 12 samples. Geochim. Cosmochim. Acta 36, 773-785.

Chappell B. W. and Green D. H. (1973) Chemical composition and petrogenetic relationships in Apollo 15 mare basalts. Earth Planet. Sci. Lett. 18, 237-246.

Compston W., Berry H., Vernon M. G., Chappell B. W., and Kaye M. (1971) Rubidium-strontium chronology and chemistry of lunar material from the Ocean of Storms. Proc. Lunar Sci. Conf. 2nd, p. 1471-1485.

Cuttitta F., Rose H. J., Annell C. S., Carron M. K., Christian R. P., Dwornik E. G., Greenland L. P., Helz A. W., and Ligon D. T. (1971) Elemental composition of some Apollo 12 lunar rocks and soil. Proc. Lunar Sci. Conf. 2nd, p. 1217-1229.

Donaldson C. H., Usselman T. M., Williams R. J., and Lofgren C. E. (1975) Experimental modeling of the cooling history of Apollo 12 olivine basalts. Proc. Lunar Sci. Conf. 6th, p. 843-869.

Duncan A. R., Erlank A. J., Sher M. K., Abraham Y. C., Willis J. P. and Ahrens L. H. (1976) Some trace element constraints on lunar basalt genesis. Proc. Lunar Sci. Conf. 7th, p. 1659-1671.

Dungan M. A. and Brown R. W. (1977) The petrology of the Apollo 12 ilmenite basalt suite (this volume).

Engel A. E. J., Engel C. G., Sutton A. L. and Myers A. T. (1971) Composition of five Apollo 11 and Apollo 12 rocks and one Apollo 11 soil and some petrogenic considerations. Proc. Lunar Sci. Conf. 2nd, Vol. 1, pp. 439-448.

Gast P. W., Hubbard N. J. and Wiesmann (1970) Chemical composition and petrogenesis of basalts from Tranquility base. Proc. Apollo 11 Lunar Sci. Conf. pp. 1143-1163.

Green D. H., Ringwood A. E., Ware N. G., Hibberson W. O., Major A. and Kiss E. (1971a) Experimental petrology and petrogenesis of Apollo 12 basalts. Proc. Lunar Sci. Conf. 2nd, p. 601-615.

Green D. H., Ware N. G., Hibberson W. O., and Major A. (1971b) Experimental petrology of Apollo 12 basalts, 1, Sample 12009. Earth Planet. Sci. Lett., 13, 85-96.

Hart S. R., Gunn B. M., Watkins N. D. (1971) Intralava variation of alkali elements in Icelandic Basalt. Am. J. Sci., 270, 315-318.

Haskin L. A., Helmke P. A., Allen R. O., Anderson M. R., Korotev R. L. and Zweifel K. A. (1971) Rare-earth elements in Apollo 12 lunar materials. Proc. Lunar Sci. Conf. 2nd, Vol. 2, pp. 1307-1317.

Helmke P. A., Blanchard D., Haskin L., Telander K., Weiss C. and Jacobs J. (1973) Major and trace elements in rocks from Apollo 15. The Moon, 8, 129-148.

Howard K. A., Head J. W. and Swann G. A. (1972) Geology of Hadley Rille. Proc. Lunar Sci. Conf. 3rd, p. 1-14.

Hubbard N. J. and Gast P. W. (1971) Chemical composition and origin of non-mare lunar basalts. Proc. Lunar Sci. Conf. 2nd, Vol. 2, pp. 999-1020.

Jacobs J. W., Korotev R. L., Blanchard D. P. and Haskin L. A. (1976) A well tested procedure for instrumental neutron activation analysis of silicate rocks and minerals. J. Radioanal. Chem.

James O. B. and Wright T. L. (1972) Apollo 11 and 12 mare basalts and gabbros: Classification, compositional variations, and possible petrogenetic relations. Geol. Soc. Amer. Bull. 83, 2357-2382.

Kushiro I. and Haramura H. (1971) Major element variation and possible source materials of Apollo 12 crystalline rocks. Science 171, 1235-1237.

Lofgren G., Donaldson C. H., Williams R. J., Mullins O., Jr., and Usselman T. M. (1974) Experimentally reproduced textures and mineral chemistry of Apollo 15 quartz normative basalts. Proc. Lunar Sci. Conf. 5th, p. 447-469.

LSPET (Lunar Sample Preliminary Examination Team) (1970) Preliminary examination of Lunar samples from Apollo 12, Science 167, p. 1325-1339.

Maxwell, J. A. and Wiik, H. B. (1971) Chemical composition of Apollo 12 lunar samples 12004, 12033, 12051, 12052, 12065. Earth Planet. Sci. Lett., 10, p. 285.

McGetchin T. R., Settle M., and Head J. W. (1973) Radial thickness variation in impact crater ejecta: implications for lunar basin deposits. Earth Planet. Sci. Lett. 20, 226-236.

Norrish K. and Chappell B. W. (1967) X-ray fluorescence spectrography. In Physical Methods in Determinative Mineralogy (editor J. Zussman), pp. 161-214, Academic Press.

Norrish K. and Hutton J. T. (1969) An accurate X-ray spectrographic method for the analysis of a wide range of geological samples. Geochim. Cosmochim. Acta 33, 431-453.

Nyquist L. E., Bansal B. M. Wooden J. L., and Wiesmann H. (1977) Sr-Isotopic Comstraints on the petrogeneis of Apollo 12 mare basalts (this volume).

Papanastassiou D. A., and G. J. Wasserburg (1971) Lunar chronology and evolution from Rb-Sr studies of Apollo 11 and 12 samples. Earth Planet. Sci. Lett., 11, 37-62.

Papike J. G., Hodges F. N., Bence A. E., Cameron M., and Rhodes J. M., (1976) Mare Basalts: Crystal Chemistry, Mineralogy, and Petrology. Rev. Geophys. Space. Phys. 14, p. 475-540.

Pieters C. and McCord T. B. (1976) Characterization of lunar mare basalt types: I. A remote sensing study using reflection spectroscopy of surface soils. Proc. Lunar Sci. Conf. 7th, p. 2677-2690.

Rhodes J. M. and Hubbard N. J. (1973) Chemistry, classification and petrogenesis of Apollo 15 mare basalts. Proc. Lunar Sci. Conf. 4th, p. 1127-1148.

Rhodes J. M., Hodges F. N., and Papike J. J. (1975) Major element composition and classification, in Papers Presented to the Conference on Origins of Mare Basalts and Their Implications for Lunar Evolution, pp. 135-139. Lunar Science Institute, Houston.

Rhodes J. M., Hubbard N. J., Wiesmann H., Rodgers K. V., Brannon J. C. and Bansal B. M. (1976) Chemistry, classification and petrogeneis of Apollo 17 mare basalts. Proc. Lunar Sci. Conf. 7th, p. 1467-1489.

Roeder P. L. and Emslie P. F. (1970) Olivine-liquid equilibrium. Contr. Mineral. and Petrol. 29, 275-289.

Schaber G. G., Boyce J. M., and Moore H. J. (1976) The scarcity of mappable flow lobes on the lunar maria: Unique morphology of the Imbrium flows. Proc. Lunar Sci. Conf. 7th, p. 2783-2800.

Schnetzler C. C. and Philpotts J. A. (1971) Alkali, alkaline earth, and rare-earth element concentrations in some Apollo 12 soils, rocks, and separated phases. Proc. Lunar Sci. Conf. 2nd, p. 1101-1122.

Scoon G. H. (1971) Chemical analyses of lunar samples 12040 and 12064. Proc. Lunar Sci. Conf. 2nd, p. 1259-1260.

Shih C-Y., Haskin L. A., Wiesmann H., Bansal B. M. and Brannon J. C. (1975) On the origin of high-Ti mare basalts. Proc Lunar Sci. Conf. 6th, p. 1255-1285.

Sutton R. L. and Schaber G. G. (1971) Lunar locations and orientations of rock samples from Apollo missions 11 and 12. Proc. Lunar Sci. Conf. 2nd, p. 17-26.

Wanke H., Wlotzka F., Baddenhausen H., Balacescu A., Spettel B., Teschke F., Jagoutz E., Kruse H., Quijano-Rico M., and Rieder R. (1971) Apollo 12 samples: Chemical composition and its relation to sample locations and exposure ages, the two component origin of the various soil samples and studies on lunar metallic particles. Proc. Lunar Sci. Conf. 2nd, p. 1187-1208.

Walker D., Longhi J., Kirkpatrick R. J. and Hays J. F. (1976a) Differentiation of an Apollo 12 picrite magma. Proc. Lunar Sci. Conf. 7th, p. 1365-1389.

Walker D. R., Kirpatrick R. J. Longhi J., and Hays J. F. (1976b) Crystallization history of lunar picritic basalt sample 12002: Phase-equilibria and cooling-rate studies. Geol. Soc. Amer. Bull., 87, 646-656.

Warner J. L. (1971) Lunar crystalline rocks: Petrology and geology. Proc. Lunar Sci. Conf. 2nd, p. 469-480.

Weill D. F., Grieve R. A., McCallum I. S., Bottinga Y. (1971) Mineralogy-petrology of lunar samples. Microprobe studies of samples 12021 and 12022; viscosity of melts of selected lunar compositions. Proc. Lunar Sci. Conf. 2nd, p. 413-430.

Willis J. P., Ahrens L. H., Danchin R. V., Erlank A. J., Gurney J. J. Hofmeyr P. K., McCarthy T. S. and Orren M. J. (1971) Some interelement relationships between lunar rocks and fines, and stony meteorites. Proc. Lunar Sci. Conf. 2nd, p. 1123-1138.

Table 1.- Major and trace element chemistry of mare basalts

	Olivine basalts				
	12006,16	12012,15	12014,17	12076,18	12015,9-11
Major Elements (wt. %)					
SiO_2	44.23	44.17	45.34	44.87	44.98
TiO_2	2.59	2.64	2.68	2.76	2.86
Al_2O_3	7.67	7.71	8.00	8.10	8.57
FeO	20.94	20.69	20.33	20.66	20.18
MnO	9.29	0.30	0.26	0.30	0.29
MgO	14.67	14.37	13.85	12.26	11.88
CaO	8.13	8.47	8.63	9.03	9.21
Na_2O	0.20	0.21	0.21	0.21	0.23
K_2O	0.05	0.06	0.06	0.06	0.06
P_2O_5	0.05	0.09	0.05	0.03	0.06
S	0.06	0.07	0.07	—	0.07
Cr_2O_3	0.91	0.69	0.64	0.68	0.68
Total	99.59	99.47	100.12	98.94	99.07
Mg' value	55.5	55.3	54.8	51.4	51.2
Normative olivine or quartz	0 20.5	0 20.2	0 14.9	0 12.0	0 10.1
Trace elements (ppm)					
Sr	89	89	93	94	94
Ba	56	56	53	59	61
Ce	15.7	13.8	14.7		16.3
Sm	3.77	4.02	4.14	4.03	4.31
Eu	0.72	0.76	0.75		0.81
Tb	1.02	1.17	1.01		1.05
Yb	3.3	3.4	3.3	3.4	3.7
Lu	0.47	0.47	0.53	0.51	0.53
Y	31	33	32		35
Zr	97	99	101		110
Nb	6.4	6.6	6.8		6.6
Hf	3.0	3.4	3.3		3.5
Sc	40.1	41.9	42.8	46.4	46.1
Cr	6250	4780	4450	4640	4600
Co	60	56	54	54	51
Ni	110	60	40		50

Table 1.- (Continued)

	Pigeonite basalts					
	12011,15	12043,2	12017,36	12055,25	12007,4	12039,26
Major Elements (wt. %)						
SiO_2	46.63	46.77	47.27	47.00	46.42	46.09
TiO_2	3.29	3.38	3.37	3.52	3.90	4.46
Al_2O_3	9.77	10.09	10.02	10.15	11.28	10.52
FeO	19.53	19.50	19.72	19.54	19.05	20.32
MnO	9.29	0.29	0.29	0.29	0.28	0.29
MgO	8.26	7.68	7.63	7.46	5.86	5.75
CaO	10.63	10.96	10.97	11.10	11.52	11.67
Na_2O	0.25	0.27	0.27	0.27	0.32	0.29
K_2O	0.06	0.06	0.09	0.07	0.08	0.10
P_2O_5	0.07	0.06	0.09	0.07	0.10	0.09
S	0.06	0.07	0.03	0.07	0.10	0.11
Cr_2O_3	0.59	0.50	0.52	0.47	0.28	0.38
Total	99.42	99.63	100.47	100.01	99.19	100.07
Mg' value	43.0	41.3	40.8	40.5	35.4	3.5
Normative olivine or quartz	Q 2.0	Q 2.4	Q 2.6	Q 2.8	Q 35.4	Q 3.5
Trace elements (ppm)						
Sr	113	117	118	121	142	122
Ba	71	73	75	69	91	88
Ce	19.9	17.7		18.2	23.6	25.7
Sm	5.0	5.25	5.1	5.25	6.4	6.55
Eu	0.95	1.00		0.95	1.20	1.18
Tb	1.06	1.25		1.02	1.48	1.66
Yb	4.2	4.4	4.4	4.4	5.3	5.5
Lu	0.62	0.63	0.66	0.67	0.77	0.81
Y	39	40		43	51	52
Zr	128	123		131	156	156
Nb	7.4	7.5		8.5	10.0	10.7
Hf	3.7	4.0		5.2	6.4	4.7
Sc	52.2	52.4	52.8	54.0	52.3	56.0
Cr	4050	3300	3550	3200	1980	2500
Co	39	37	32	38	26	28
Ni	n.d.	n.d.		n.d.	n.d.	n.d.

Table 1.- (Continued)

	Feldspathic basalt	Ilmenite basalts			
	12031,23	12005,7	12036,24	12008,48	12016,9
Major Elements (wt. %)					
SiO_2	46.97	41.56	43.11	42.75	42.78
TiO_2	2.88	2.76	3.20	4.45	4.02
Al_2O_3	12.63	5.30	6.16	7.98	7.23
FeO	16.78	22.27	21.82	21.94	22.64
MnO	0.26	0.30	0.30	0.30	0.30
MgO	7.13	19.97	16.71	12.33	12.65
CaO	12.25	6.31	7.46	8.97	8.42
Na_2O	0.33	0.16	0.18	0.25	0.22
K_2O	0.05	0.04	0.06	0.05	0.06
P_2O_5	0.05	0.04	0.02	0.07	0.08
S	0.05	0.04	0.07	0.08	0.08
Cr_2O_3	0.35	0.75	0.72	0.61	0.57
Total	99.73	99.50	99.81	99.78	99.05
Mg' value	43.1	61.5	57.7	50.0	49.9
Normative olivine or quartz	Q 2.1	O 42.0	O 28.3	O 17.5	O 18.2
Trace elements (ppm)					
Sr	136	83	91	130	126
Ba	60	35	56	51	59
Ce	15.6	10.2	14.0	16.9	16.2
Sm	4.23	2.99	4.03	5.35	5.5
Eu	1.00	0.62	0.75	1.06	1.06
Tb	1.19	0.77	0.95	1.39	1.42
Yb	3.7	2.66	3.5	4.9	5.0
Lu	0.55	0.41	0.51	0.71	0.67
Y	35	28	36	45	45
Zr	100	66	97	117	117
Nb	7.0	4.3	6.6	5.9	6.1
Hf	3.3	2.4	4.7	3.8	6.3
Sc	48.9	37.1	42.6	52.4	49.4
Cr	2460	5200	4880	4200	3950
Co	26	71	63	51	54
Ni	n.d.	90	60	n.d.	25

Table 1.- (Concluded)

	Ilmenite basalts			
	12045,12	12056, 10	12054,62	12047,3
Major Elements (wt. %)				
SiO_2	42.30	43.44	45.86	45.13
TiO_2	4.78	5.07	4.63	5.20
Al_2O_3	8.06	8.82	10.47	10.10
FeO	22.09	21.60	19.51	20.50
MnO	0.29	0.29	0.29	0.29
MgO	11.63	9.30	6.76	6.59
CaO	9.09	10.21	11.93	11.32
Na_2O	0.26	0.29	0.31	0.31
K_2O	0.07	0.07	0.07	0.08
P_2O_5	0.09	0.07	0.06	0.08
S	0.09	0.10	0.09	0.12
Cr_2O_3	0.59	0.48	0.33	0.31
Total	99.34	99.74	100.31	100.02
Mg' value	48.4	43.4	38.2	36.4
Normative olivine or quartz	O 16.3	O 6.9	Q 2.2	Q 2.2
Trace elements (ppm)				
Sr	136	159	162	171
Ba	52	62	64	69
Ce	17.4	20.2	18.8	20.1
Sm	5.6	6.4	6.0	6.5
Eu	1.19	1.31	1.27	1.36
Tb	1.51	1.73	1.85	1.80
Yb	5.1	6.0	5.8	5.9
Lu	0.73	0.82	0.78	0.89
Y	50	55	51	57
Zr	112	135	128	141
Nb	5.3	6.1	6.3	7.0
Hf	4.5	4.8	4.8	5.1
Sc	54.0	60.0	64.0	61.0
Cr	4060	3310	2300	2190
Co	52	42	31	32
Ni	40	n.d.	n.d.	n.d.

Table 2: Brief Petrographic Descriptions of Apollo 12 Mare Basalts Analyzed in this Study

Olivine Basalts

12006 - Ophitic texture lacking olivine. Abundant silica. Petrography does not agree with chemical composition, or A-12 catalogue description.

12012 - Porphyritic-subophitic. Partly resorbed olivine phenocrysts in a subophitic groundmass.

12014 - Similar to 12012.

12076 - Porphyritic. Olivine and pigeonite phenocrysts in a variolitic groundmass.

12015 - Olivine vitrophyre. Olivine phenocrysts and skeletal microphenocrysts in a rapidly quenched groundmass. Very similar to 12009.

Pigeonite Basalts

12011 - Porphyritic. Pyroxene and olivine phenocrysts in a variolitic groundmass.

12043 - Porphyritic. Large pyroxene phenocrysts and minor olivine in a groundmass that varies in texture from subophitic to variolitic.

12017 - Porphyritic. Pyroxene phenocrysts and very minor olivine in a subophitic groundmass.

12055 - Porphyritic. Large pyroxene phenocrysts and minor olivine in a groundmass that varies from variolitic to subophitic.

12007 - Microgabbro. Ophitic to graphic intergrowth of plagioclase and pyroxene plus acicular ilmenite and silica.

12039 - Microgabbro. Similar to 12007.

Table 2: (Concluded)

Ilmenite Basalts

12005 - Coarse-grained heterogeneous cumulus texture includes large oikocrysts of pyroxene and an interstitial assemblage of olivine, plagioclase and ilmenite.

12036 - Coarse-grained cumulate dominated by equant pyroxene grains. Interstitial plagioclase, olivine and ilmenite.

12008 - Olivine vitrophyre. Olivine phenocrysts and skeletal microphenocrysts in a rapidly quenched groundmass. Similar to 12009.

12016 - Medium-grained equigranular basalt. Abundant pyroxene plus partly resorbed olivine and interstitial plagioclase.

12045 - Porphyritic. Olivine and augite phenocrysts in a variolitic groundmass.

12056 - Medium-grained subophitic. Minor resorbed olivine.

12054 - Subophitic. Lacks olivine. Heavily shocked.

12047 - Equigranular Ophitic. Lacks olivine.

Feldspathic Basalt

12031 - Coarse-grained graphic intergrowth of plagioclase and pyroxene plus needles of cristobalite and ilmenite.

Table 3: Trace element ratios in Apollo 12 mare basalts

		Olivine Basalts	Pigeonite Basalts	Ilmenite Basalt	12031 Feldspathic Basalt
Ba/Sm	(1)	14.1	14.2	9.5	14.2
	(2)	12.8-14.9	13.1-14.7	8.7-10.7	—
Ce/Sm	(1)	3.8	4.0	3.2	3.7
	(2)	3.4-4.2	3.4-4.0	2.9-3.4	—
Zr/Y	(1)	3.1	3.3	2.6	2.9
	(2)	3.0-3.2	3.0-3.3	2.4-2.6	—
Zr/Nb	(1)	17	17	20	14
	(2)	15-17	15-17	15-22	—
Zr/Sr	(1)	1.2	1.1	0.9	0.7
	(2)	1.1-1.2	1.1-1.3	0.8-0.9	—
Ba/Sr	(1)	0.65	0.63	0.39	0.44
	(2)	0.57-0.65	0.57-0.72	0.38-0.47	—
Ba/Sc	(1)	1.32	1.36	0.97	1.23
	(2)	1.24-1.40	1.28-1.74	0.94-1.19	—
Sc/Sm	(1)	10.7	10.4	9.8	11.6
	(2)	10.4-11.5	8.2-10.4	9.0-12.4	—

(1) "Best estimate" for group based on most rapidly cooled sample.
(2) Range.

Table 4: Classification of Chemically Analyzed
Apollo 12 Mare Basalts

Olivine basalts	12009, 12015, 12075, 12076, 12004, 12012, 12006, 12002, 12020 12014, 12018, 12040, 12035.
Pigeonite basalts	12011, 12053, 12052, 12065, 12043, 12055, 12017, 12021, 12007, 12039, 12064.
Ilmenite basalts	12008, 12045, 12022, 12051, 12047, 12063, 12056, 12054, 12016, 12036?, 12005.
Feldspathic basalts	12031?, 12038.

FIGURE CAPTIONS

Fig. 1. Ba/Sm ratios versus atomic Mg/(Mg+Fe) values for Apollo 12 mare basalts. Rapidly cooled vitrophyres and basalts with a variolitic groundmass are represented by filled symbols, more slowly cooled samples with ophitic and gabbroic textures are represented by open symbols.

Data from Table 1 are indicated by large symbols, that from other studies by small symbols (Compston et al., 1971; Cuttita et al., 1971; Engel et al., 1971; Haskin et al., 1971; Hubbard and Gast, 1971; Kushiro and Haramura, 1971; Maxwell and Wiik, 1971; Schnetzler and Philpotts, 1971; Scoon, 1971; Wanke et al., 1971; Willis et al., 1971).

Fig. 2. Initial $^{87}Sr/^{86}Sr(I)$ versus TiO_2 for Apollo 12 mare basalts. Symbols are the same as in Fig. 1. Data from Nyquist et al., (1977) and Papanastassiou and Wasserburg (1971). The Cal-Tech data have been adjusted for inter-laboratory bias by the addition of 0.00012 in $^{87}Sr/^{86}Sr$.

Fig. 3. MgO-SiO_2 relationships in Apollo 12 mare basalts. Symbols are the same as in Fig. 1. Olivine control lines (Fo_{72}) indicating the effects of olivine addition and subtraction are shown in solid lines; olivine (Fo_{66}) control in a broken line; and pigeonite control by a dot-dash line. These control lines are for reference purposes, they are not intended as lines of "best fit." The data sources are the same as in Fig. 1.

Fig. 4. MgO-TiO_2 relationships in Apollo 12 mare basalts. Symbols and data sources are the same as in Figs. 1 and 3.

Fig. 5. TiO_2-CaO relationships in Apollo 12 mare basalts. Symbols and data sources are the same as in Figs. 1 and 3. Also shown in a dotted line is the experimentally determined liquid line of descent for 12002 (Walker et al., 1976b).

Fig. 6. MgO-Ba relationships in Apollo 12 mare basalts. Symbols are the same as in Figs. 1 and 3. Only data from this paper are shown

Fig. 7. MgO-Sm relationships for Apollo 12 mare basalts. Symbols are the same as in Figs. 1 and 3. Only data from this paper are shown.

Fig. 8. MgO-Sr relationships for Apollo 12 mare basalts. Symbols are the same as in Figs. 1 and 3, only data from this paper are shown.

Fig. 9. Sample locations at the Apollo 12 landing site. Symbols are the same as in Fig. 1.

Fig. 10. Cooling rate - differentiation relationships for Apollo 12 olivine-pigeonite basalts. The Mg/(Mg+Fe) value provides a measure of the position of samples in the fractionation sequence relative to the inferred parental magma (12015). Also shown (lower left in each box) is the normative olivine or quartz content, and (lower right) the ratio of Ba_{sample}/Ba_{12015}. Both provide additional measures of the differentiation process. Samples studied in this paper are enclosed by heavier outlines. The source of data for Mg/(Mg+Fe) values is the same as in Fig. 1; only data from Table 1 is used for the Ba_{sample}/Ba_{12015} ratio.

Fig. 11. Cooling rate-differentiation relationships for Apollo 12 ilmenite basalts. The conventions and sources of data are the same as in Fig. 10, except that the inferred parental magma is 12008.

Fig. 1

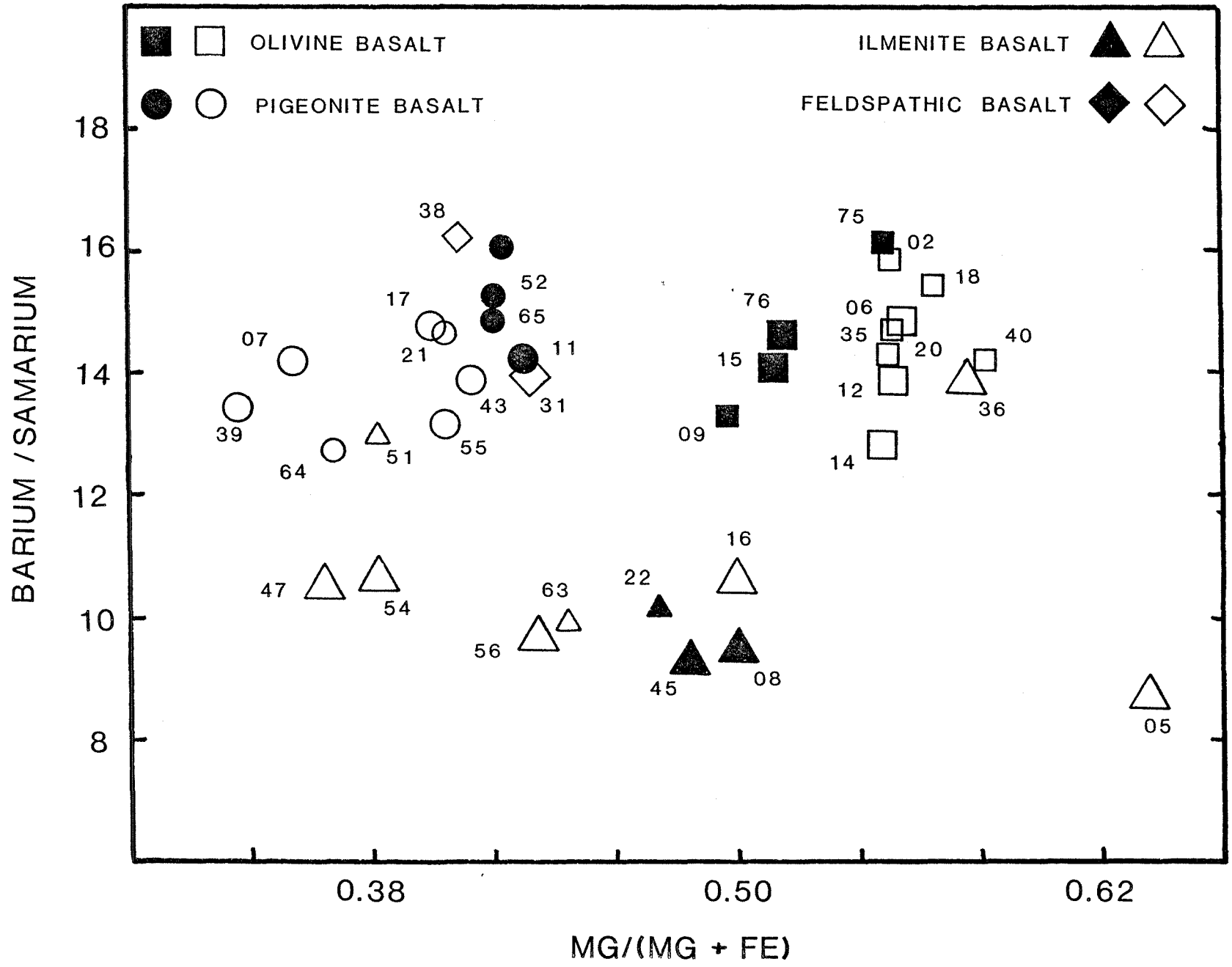
OLIVINE BASALT
ILMENITE BASALT
PIGEONITE BASALT
FELDSPATHIC BASALT
BARIUM /SAMARIUM
18
16
14
12
10
8
0.38
0.50
0.62
MG/(MG + FE)
38
52
17
65
07
21
11
43
31
39
64
51
55
75
02
18
76
06
35
20
40
15
12
36
09
14
16
47
54
63
22
56
45
08
05

Fig. 2

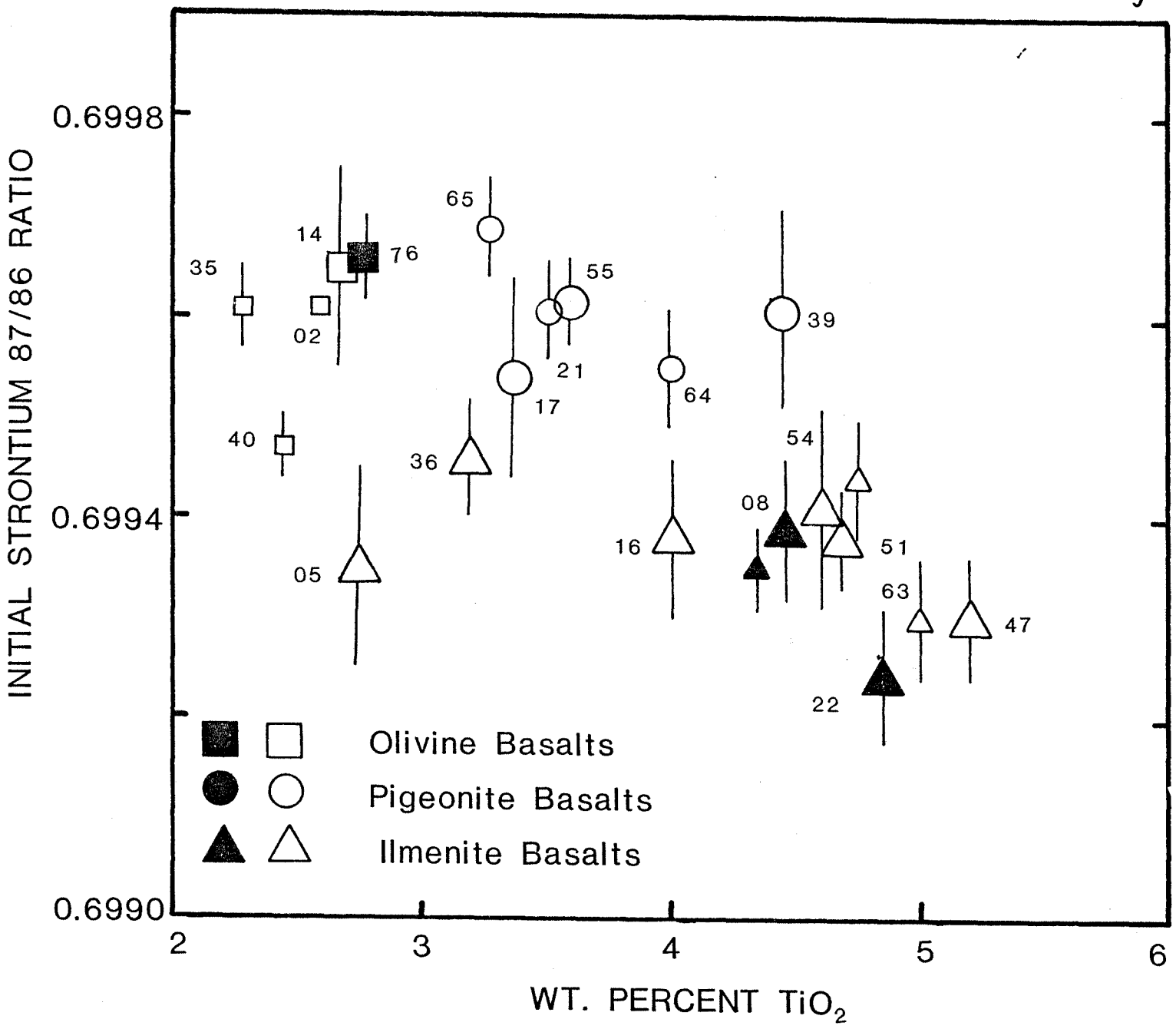
INITIAL STRONTIUM 87/86 RATIO
0.6998
0.6994
0.6990
2
3
4
5
6
WT. PERCENT TiO2
35
14
76
02
65
55
39
21
17
64
40
36
54
08
16
51
05
63
47
22
Olivine Basalts
Pigeonite Basalts
Ilmenite Basalts

Fig. 3

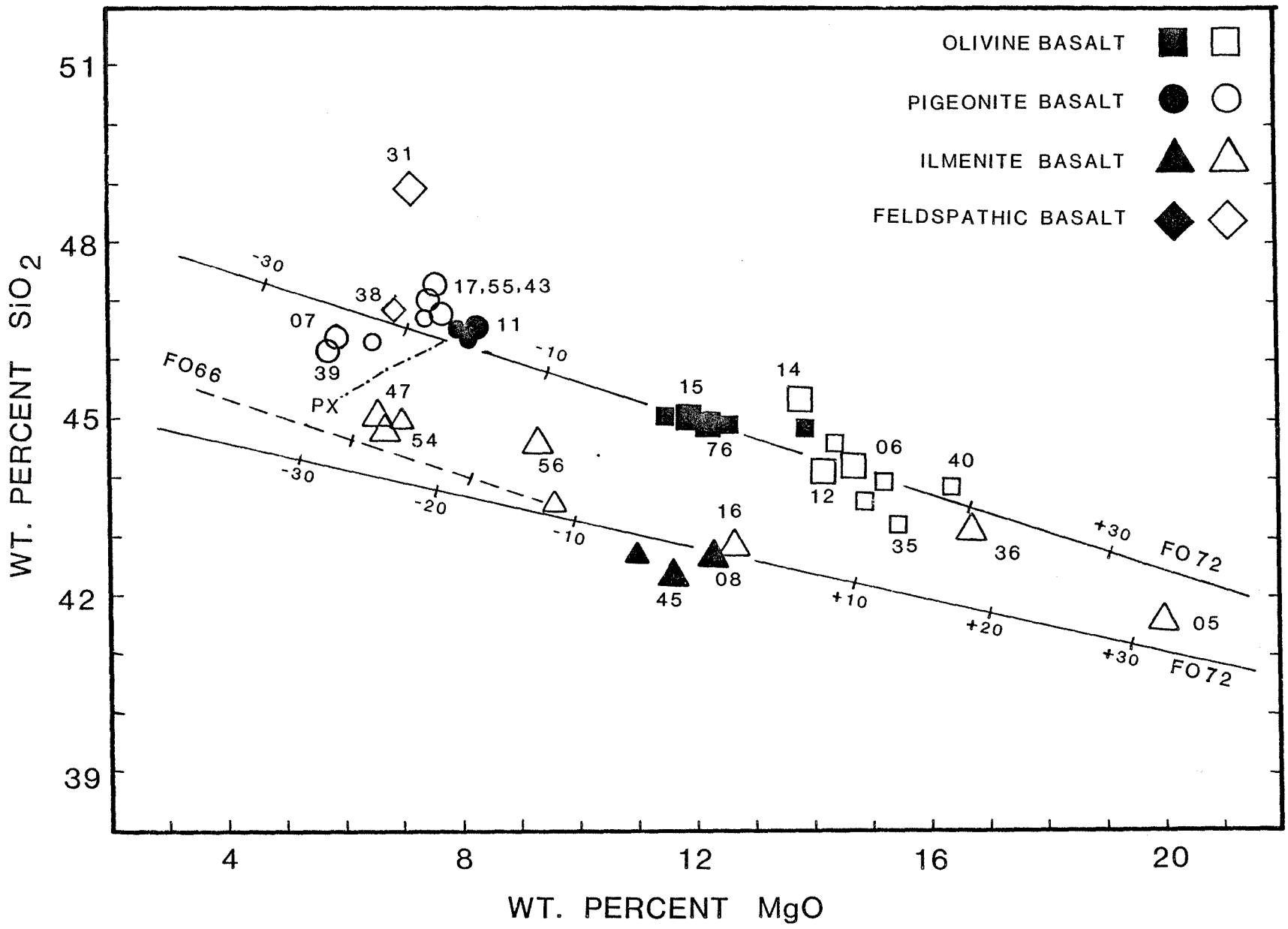
OLIVINE BASALT
PIGEONITE BASALT
ILMENITE BASALT
FELDSPATHIC BASALT
WT. PERCENT SiO2
WT. PERCENT MgO
51
48
45
42
39
4
8
12
16
20
31
38
17,55,43
07
11
39
-30
-10
FO66
PX
47
54
56
15
76
14
06
40
12
35
36
+30
FO72
16
08
45
-30
-20
-10
+10
+20
+30
FO72
05

Fig. 4

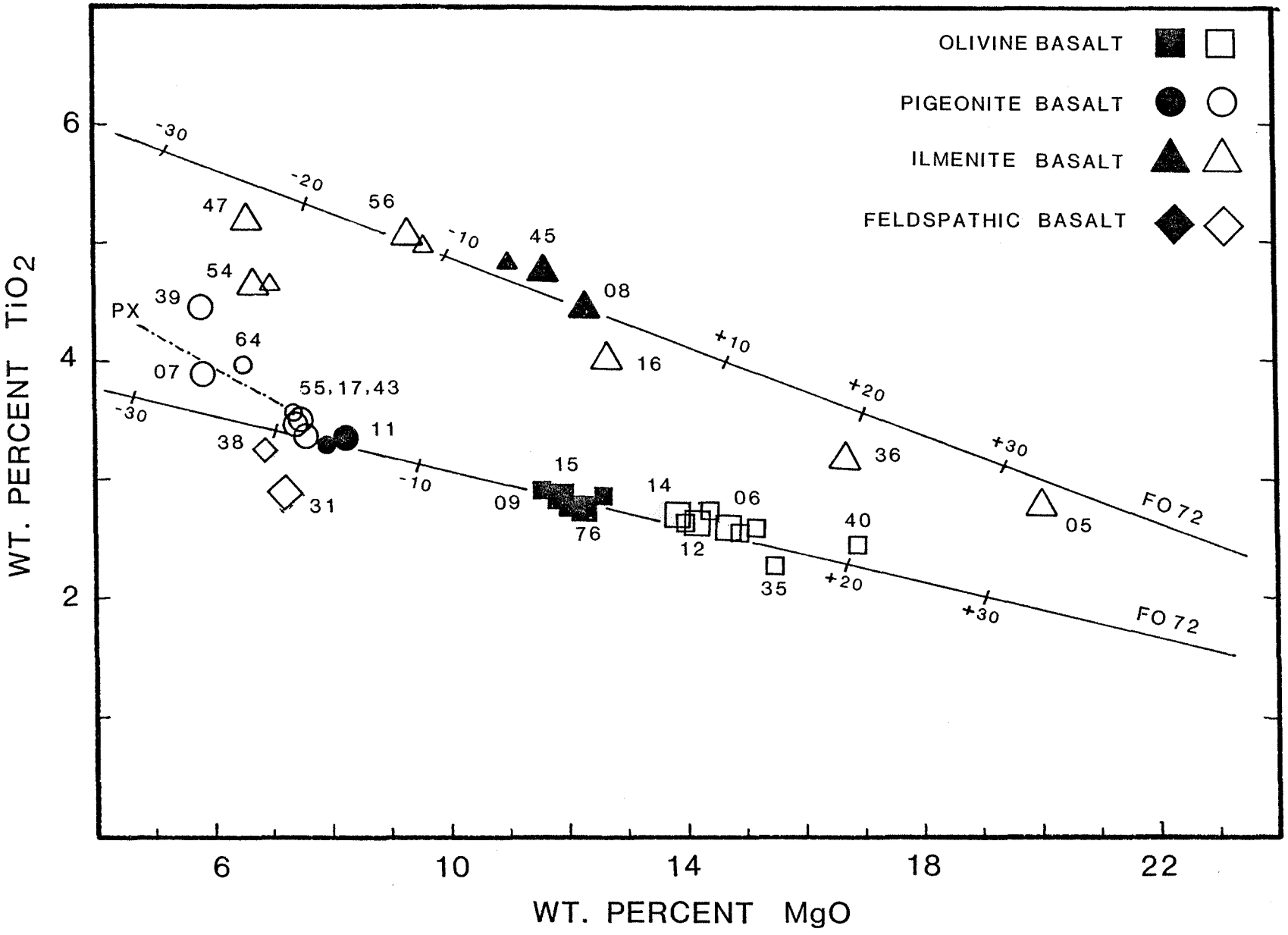
OLIVINE BASALT
PIGEONITE BASALT
ILMENITE BASALT
FELDSPATHIC BASALT
WT. PERCENT TiO2
WT. PERCENT MgO
6
4
2
6
10
14
18
22
-30
-20
-10
+10
+20
+30
FO 72
FO 72
PX
47
56
45
54
39
08
64
07
16
55,17,43
11
38
36
15
09
14
06
40
31
76
12
35
05

Fig. 5

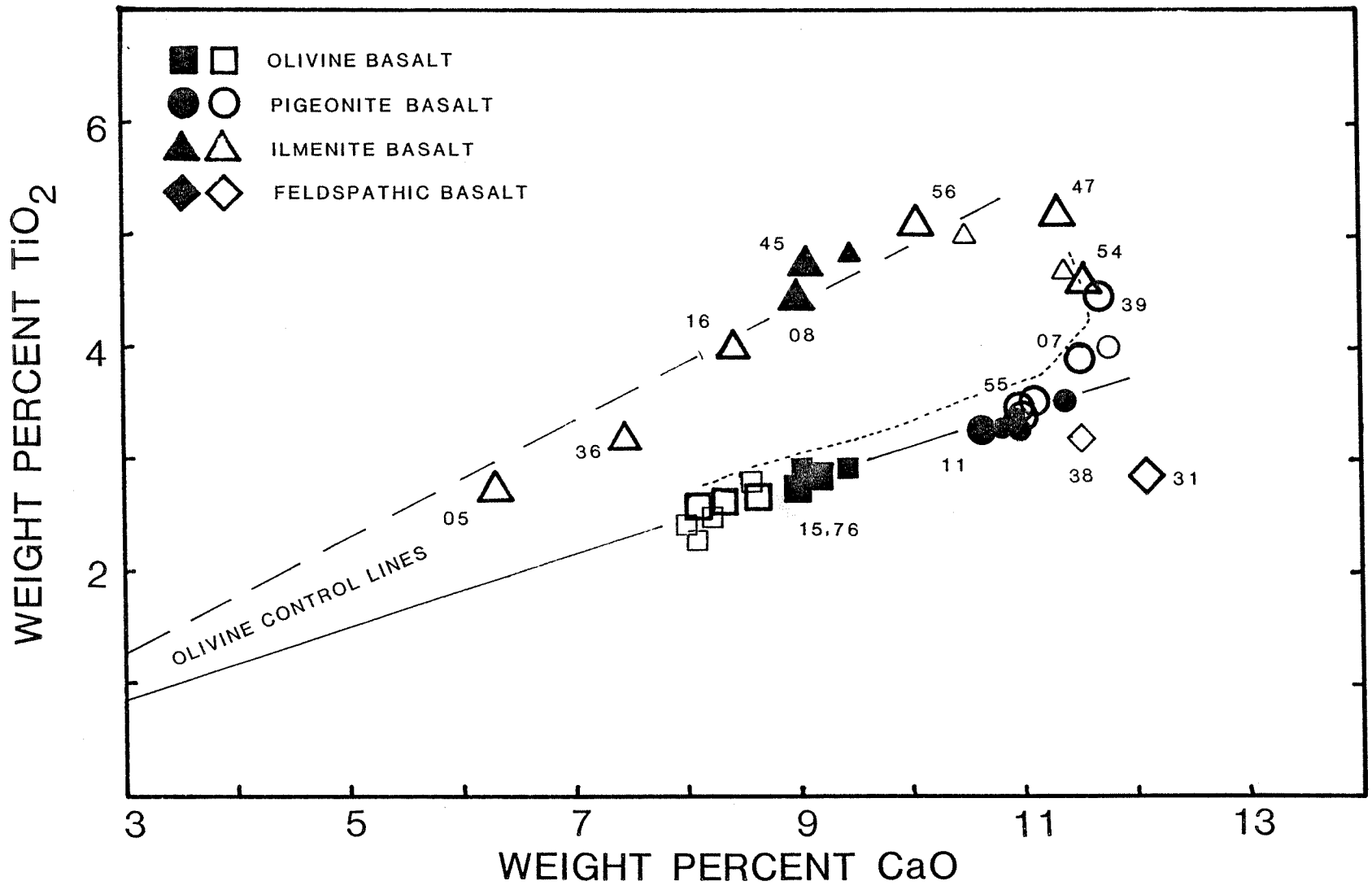
OLIVINE BASALT
PIGEONITE BASALT
ILMENITE BASALT
FELDSPATHIC BASALT
WEIGHT PERCENT TiO_2
WEIGHT PERCENT CaO
OLIVINE CONTROL LINES
2
4
6
3
5
7
9
11
13
05
16
36
45
08
56
47
54
39
07
55
11
38
31
15,76

Fig. 6

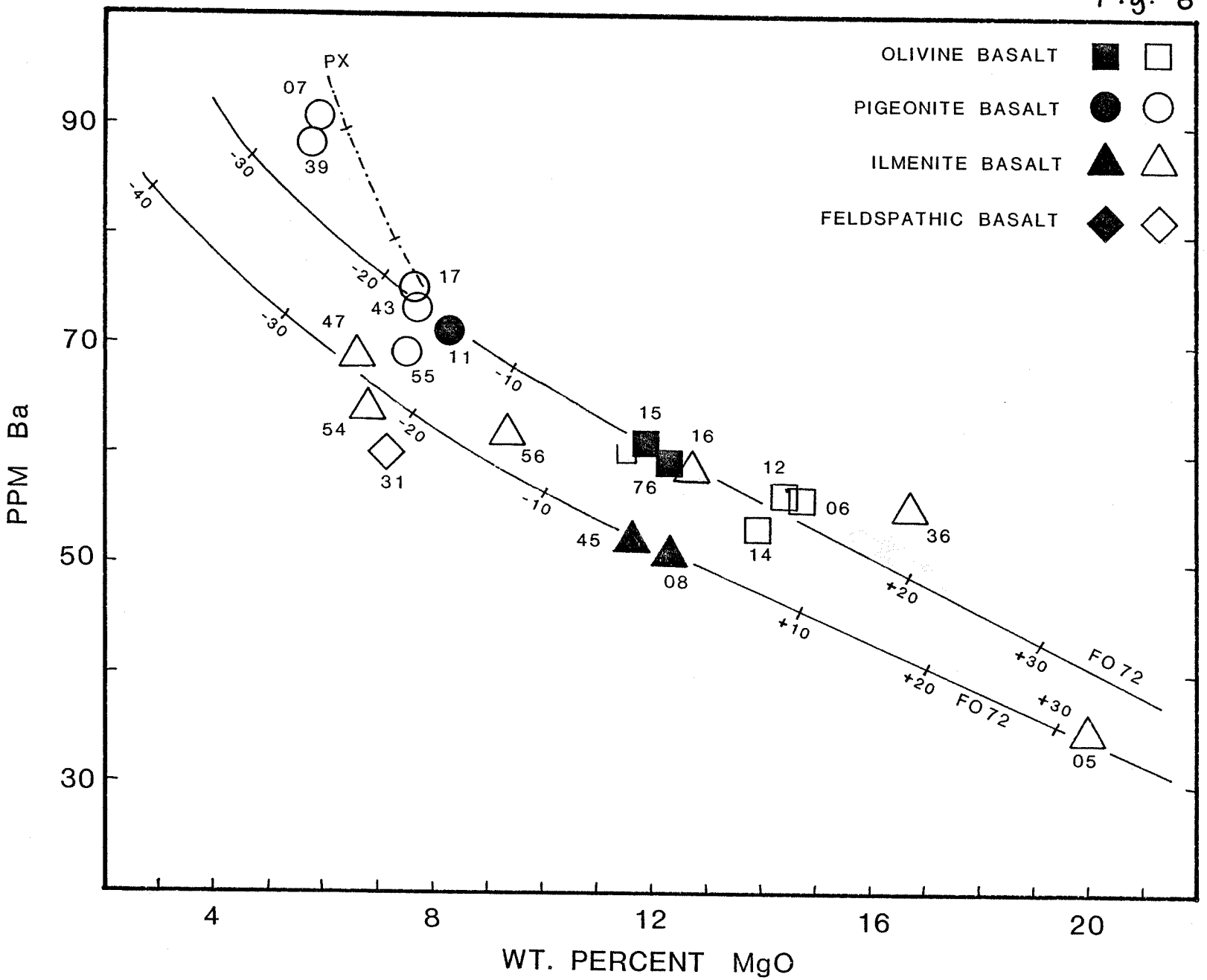
OLIVINE BASALT
PIGEONITE BASALT
ILMENITE BASALT
FELDSPATHIC BASALT
PX
07
39
17
43
11
47
55
54
31
56
15
16
76
12
06
14
36
45
08
05
-30
-40
-20
-10
+10
+20
+30
FO 72
FO 72
90
70
50
30
PPM Ba
4
8
12
16
20
WT. PERCENT MgO

Fig. 7

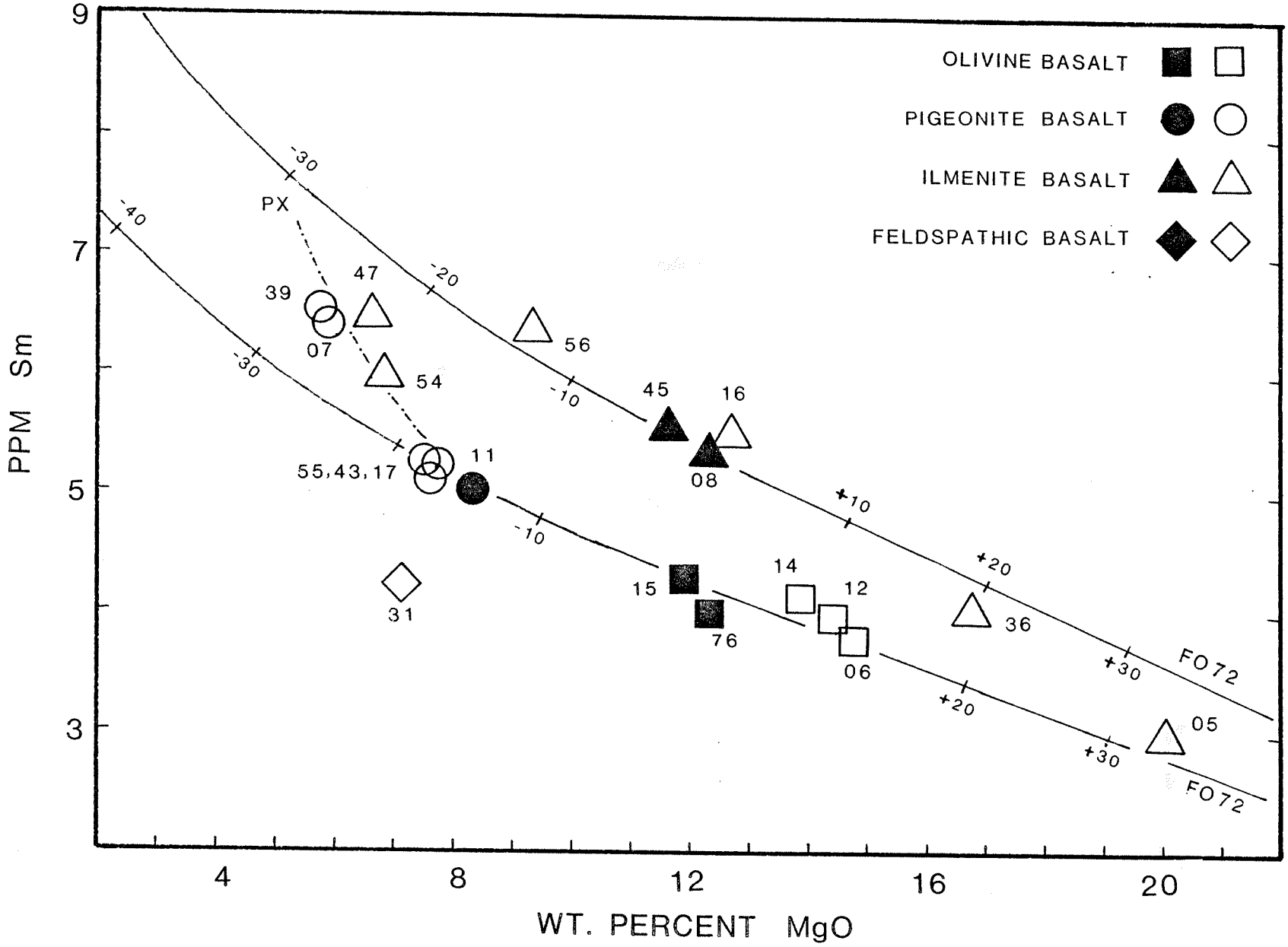
OLIVINE BASALT
PIGEONITE BASALT
ILMENITE BASALT
FELDSPATHIC BASALT
PPM Sm
WT. PERCENT MgO
9
7
5
3
4
8
12
16
20
PX
-30
-40
-20
-10
+10
+20
+30
FO72
FO72
39
47
07
54
56
45
16
08
55,43,17
11
31
15
76
14
12
06
36
05

Fig. 8

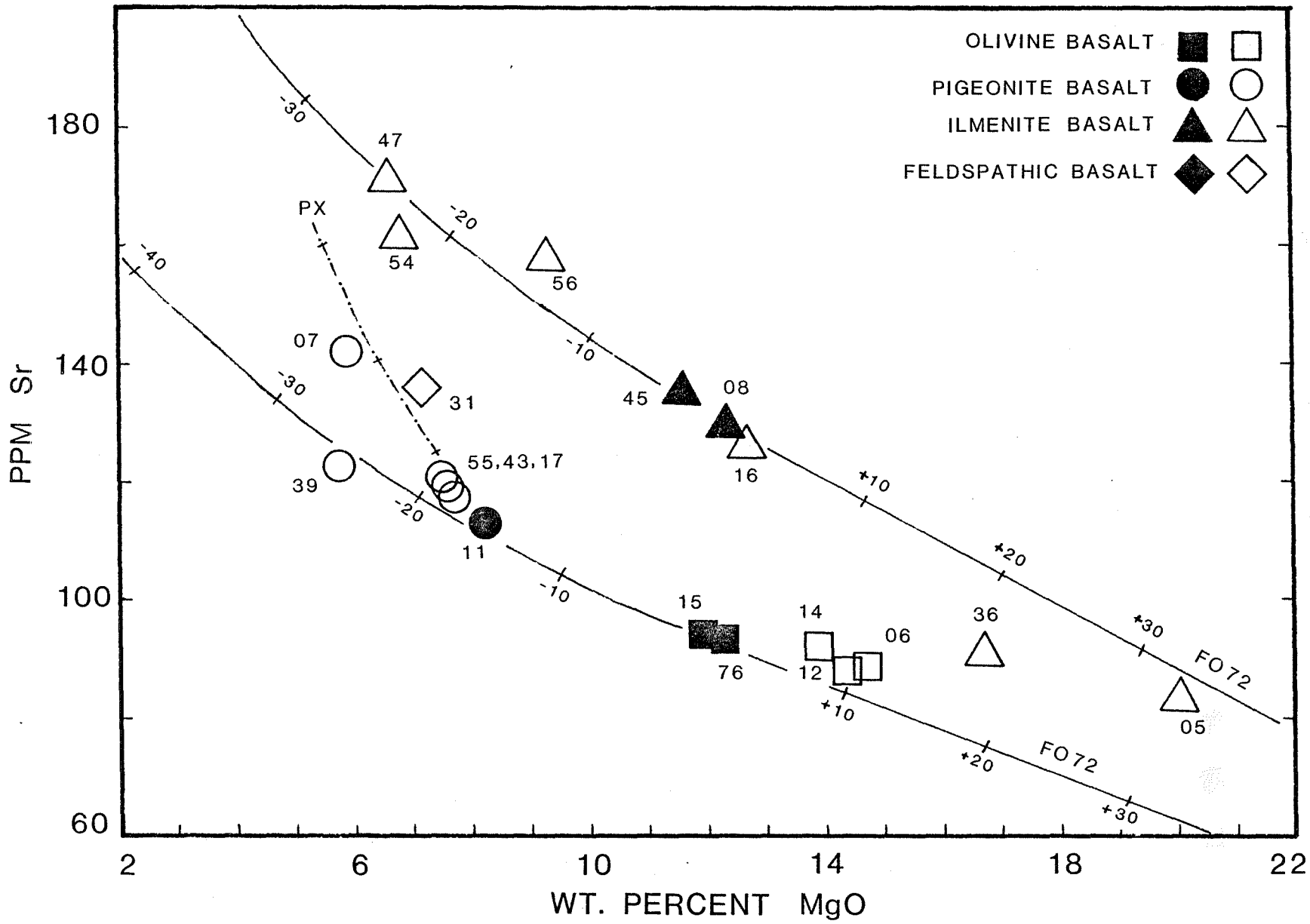
OLIVINE BASALT
PIGEONITE BASALT
ILMENITE BASALT
FELDSPATHIC BASALT
PPM Sr
180
140
100
60
2
6
10
14
18
22
WT. PERCENT MgO
PX
-40
-30
-20
-10
+10
+20
+30
FO72
FO72
47
54
56
45
08
16
05
07
31
39
55,43,17
11
15
76
14
12
06
36

Fig. 9

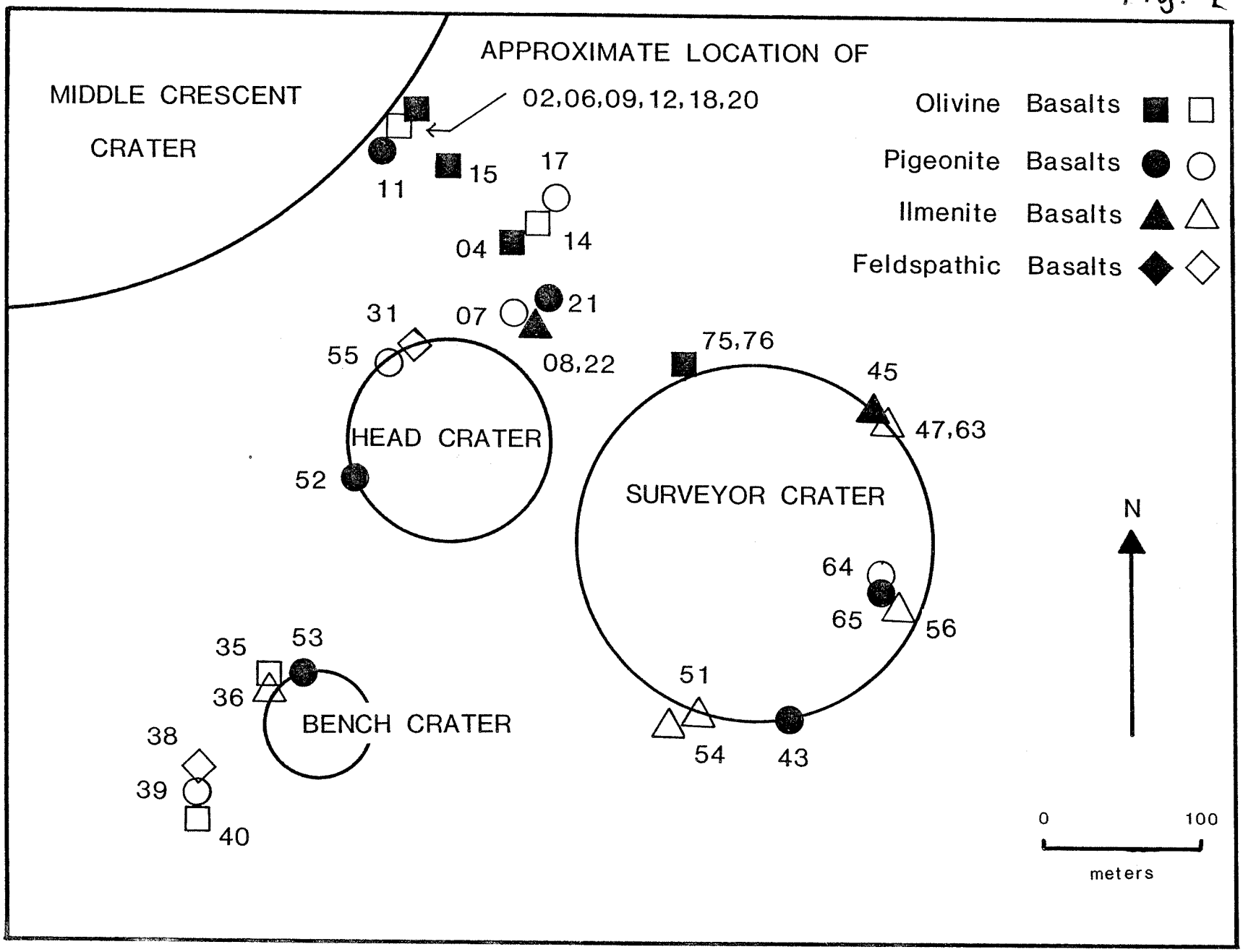
APPROXIMATE LOCATION OF
02,06,09,12,18,20
MIDDLE CRESCENT
CRATER
Olivine Basalts
Pigeonite Basalts
Ilmenite Basalts
Feldspathic Basalts
11
15
17
04
14
31
07
21
55
08,22
75,76
45
47,63
HEAD CRATER
52
SURVEYOR CRATER
64
65
56
35
53
36
BENCH CRATER
51
38
39
54
43
40
N
0
100
meters

Fig. 10

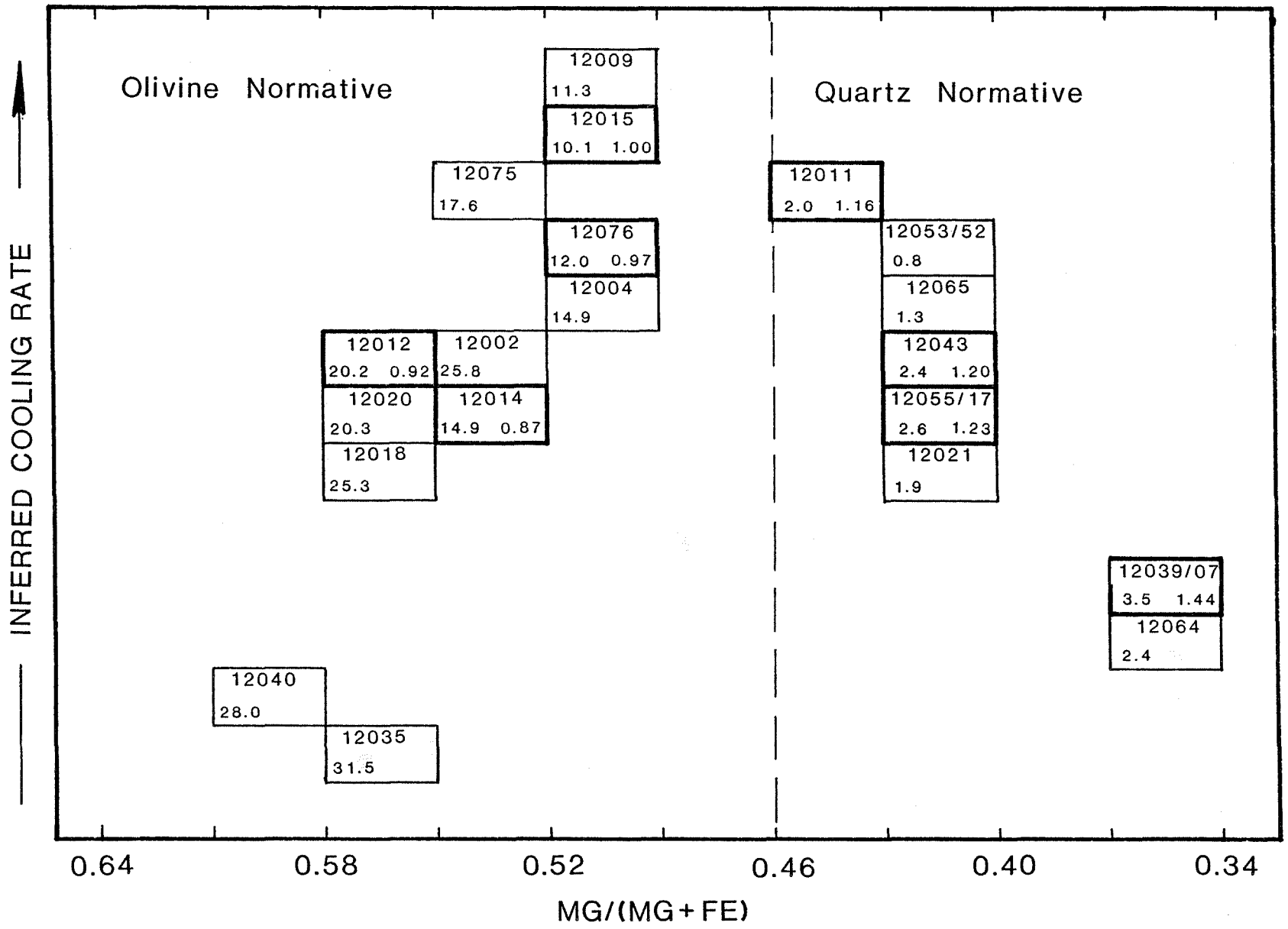
Olivine Normative
Quartz Normative
INFERRED COOLING RATE
12009
11.3
12015
10.1 1.00
12075
17.6
12076
12.0 0.97
12004
14.9
12012
20.2 0.92
12002
25.8
12020
20.3
12014
14.9 0.87
12018
25.3
12040
28.0
12035
31.5
12011
2.0 1.16
12053/52
0.8
12065
1.3
12043
2.4 1.20
12055/17
2.6 1.23
12021
1.9
12039/07
3.5 1.44
12064
2.4
0.64
0.58
0.52
0.46
0.40
0.34
MG/(MG+FE)

Fig. 11

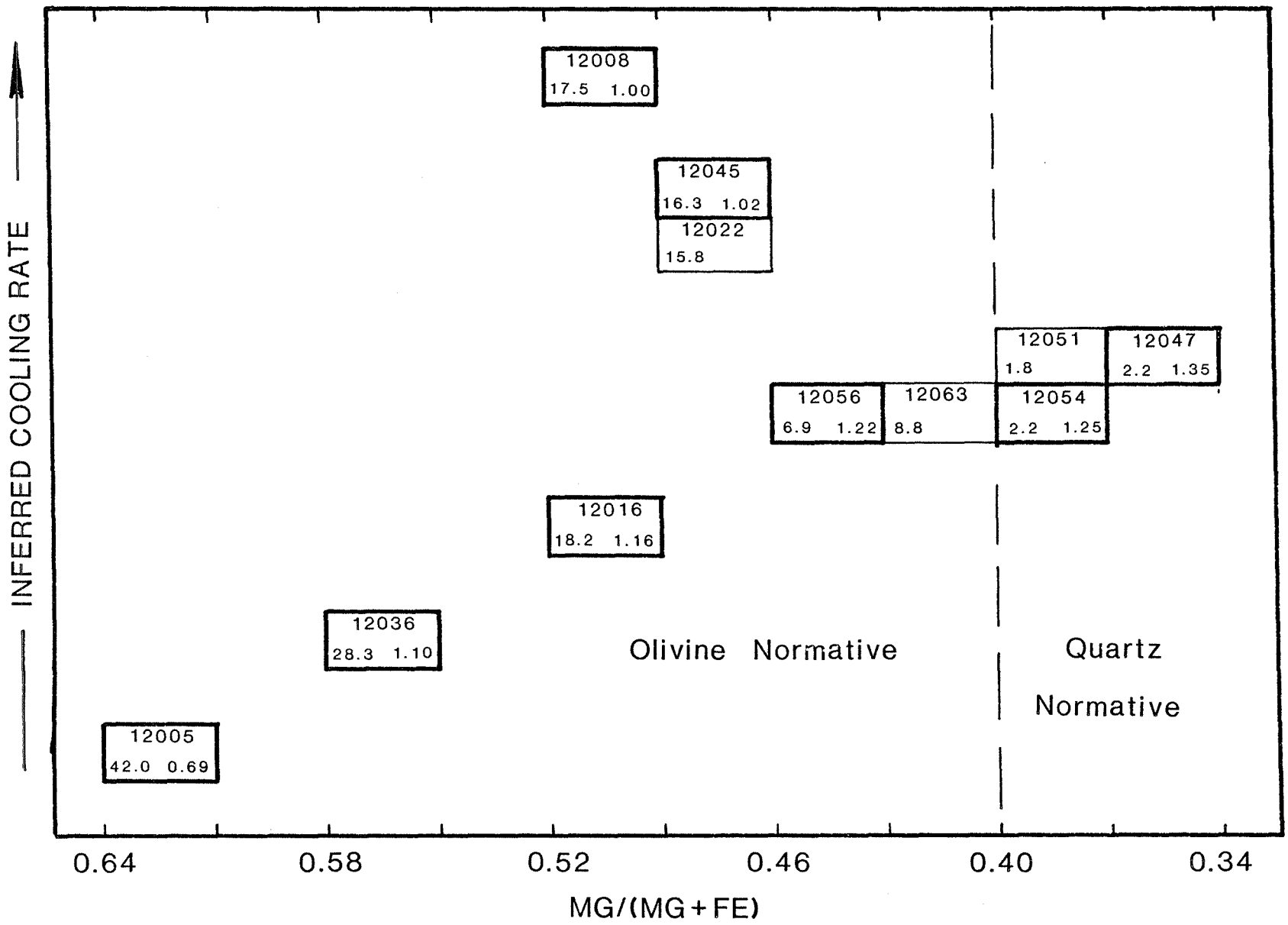
12008
17.5 1.00
12045
16.3 1.02
12022
15.8
12051
1.8
12047
2.2 1.35
12056
6.9 1.22
12063
8.8
12054
2.2 1.25
12016
18.2 1.16
12036
28.3 1.10
12005
42.0 0.69
Olivine Normative
Quartz
Normative
INFERRED COOLING RATE
0.64
0.58
0.52
0.46
0.40
0.34
MG/(MG+FE)